Chiral tunneling in single-layer and bilayer graphene

2012 Phys. Scr. 2012 014010

(http://iopscience.iop.org/1402-4896/2012/T146/014010)

IOP Publishing Physica Scripta
Phys. Scr. **T146** (2012) 014010 (17pp) doi:10.1088/0031-8949/2012/T146/014010

Chiral tunneling in single-layer and bilayer graphene

T Tudorovskiy, K J A Reijnders and M I Katsnelson

Radboud University Nijmegen, Institute for Molecules and Materials, Heyendaalseweg 135, 6525 AJ Nijmegen, The Netherlands

E-mail: m.katsnelson@science.ru.nl

Received 18 April 2011
Accepted for publication 8 June 2011
Published 31 January 2012
Online at stacks.iop.org/PhysScr/T146/014010

Abstract
In this paper, we review chiral (Klein) tunneling in single-layer and bilayer graphene and present its semiclassical theory, including the Berry phase and the Maslov index. The peculiarities of chiral tunneling are naturally explained in terms of the classical phase space. In one-dimensional geometry, we reduced the original Dirac equation, describing the dynamics of charge carriers in single-layer graphene, to an effective Schrödinger equation with a complex potential. This allowed us to study tunneling in detail and obtain analytical formulae. Our predictions are compared with numerical results. We have also demonstrated that for the case of an asymmetric n–p–n junction in single-layer graphene, there is total transmission only for normal incidence; side resonances are suppressed.

PACS numbers: 72.80.Vp, 03.65.Sq, 03.65.Pm

(Some figures may appear in colour only in the online journal)

1. Introduction

Since this paper is prepared for the proceedings of the Nobel symposium on graphene, we do not start with general explanations of what graphene is and why it is important; these are described very well in other presentations (see the reviews [1–7]). Our specific subject is chiral or Klein (as it was called in [8]) tunneling. This is one of the key phenomena determining the peculiar electronic properties of graphene. In light of possible applications, Klein tunneling protects high charge carrier mobility despite unavoidable inhomogeneities. At the same time, due to Klein tunneling, graphene electronics cannot copy the standard semiconductor one: if you make a graphene transistor based on the n–p–n junction just like for silicon, it will not be efficient since you will not be able to lock it. These two remarks illustrate the importance of the subject; a more detailed discussion is presented below.

The paper consists of two parts. The first part (sections 2–5) follows the historical lines of thought and presents the motivation for the problem, from [9] to [8]. In the second part (sections 6–12), we present a systematic semiclassical theory of chiral tunneling, together with numerical results.

2. The Klein paradox

Soon after the discovery of the Dirac equation, Klein [9] noticed one of its strange properties that was afterwards called the 'Klein paradox'. Klein considered the original 4×4 Dirac equation, which governs the dynamics of a spin-1/2 particle moving in three-dimensional (3D) space. To make a direct connection to the case of graphene without changing the essence of the paradox, we will consider a 2×2 matrix equation for a particle propagating in 2D space:

$$\hat{H}\Psi = E\Psi, \tag{1}$$

where $\Psi = (\psi_1, \psi_2)$ and the Hamiltonian

$$\hat{H} = c\,\boldsymbol{\sigma}\hat{\boldsymbol{p}} + u(x, y) + mc^2\hat{\sigma}_z. \tag{2}$$

Here m is the mass of the particle, c is the speed of light and $u(x, y)$ is the potential energy.

To demonstrate the essence of the paradox, we consider normal incidence on a 1D potential barrier, which means that $u = u(x)$ and $\psi_i = \psi_i(x)$. Then equation (1) takes the form

$$\begin{cases} -\mathrm{i}\hbar c\dfrac{\mathrm{d}\psi_2}{\mathrm{d}x} = (E - mc^2 - u(x))\psi_1, \\ -\mathrm{i}\hbar c\dfrac{\mathrm{d}\psi_1}{\mathrm{d}x} = (E + mc^2 - u(x))\psi_2. \end{cases} \tag{3}$$

To make the problem exactly solvable, we use a stepwise potential

$$u(x) = \begin{cases} 0, & x < 0, \\ u_0, & x > 0, \end{cases} \tag{4}$$

where u_0 is a positive constant. We consider a general scattering problem with an incoming wave $\Psi_{\rm in}(x)$ and a reflected wave $\Psi_{\rm r}(x)$ for $x < 0$,

$$\Psi(x) = \Psi_{\rm in}(x) + r\Psi_{\rm r}(x), \tag{5}$$

and a transmitted wave $\Psi_t(x)$ for $x > 0$,

$$\Psi(x) = t\Psi_t(x). \tag{6}$$

The x-dependence of the solutions for $x < 0$ can be written as $\exp(\pm {\rm i}kx)$, where the wave vector k satisfies the relativistic dispersion relation $E^2 = \hbar^2c^2k^2 + m^2c^4$ as can be found by diagonalizing equation (3) with $u = 0$. Alternatively, the wave vector can be written as

$$k = \frac{\sqrt{E^2 - m^2c^4}}{\hbar c}. \tag{7}$$

One can easily see that there are three distinct regimes, two of which are classically allowed, namely $E > mc^2$ corresponding to electron states and $E < -mc^2$ corresponding to hole or positron states. There is also a classically forbidden region $-mc^2 < E < mc^2$ where the wave vector k is imaginary and we have evanescent waves. In what follows, we will assume that we are in the electron regime. By calculating eigenvectors of equation (3), one obtains for the wavefunctions to the left of the barrier

$$\Psi_{\rm in}(x) = \begin{pmatrix} 1 \\ \alpha \end{pmatrix} {\rm e}^{{\rm i}kx} \tag{8}$$

and

$$\Psi_r(x) = \begin{pmatrix} 1 \\ -\alpha \end{pmatrix} {\rm e}^{-{\rm i}kx}, \tag{9}$$

where

$$\alpha = \sqrt{\frac{E - mc^2}{E + mc^2}}. \tag{10}$$

To the right of the barrier, we have a new wave vector q, which satisfies the relativistic dispersion relation $(E - u_0)^2 = \hbar^2c^2q^2 + m^2c^4$, or

$$q = \frac{\sqrt{(u_0 - E)^2 - m^2c^4}}{\hbar c}. \tag{11}$$

Consider a jump

$$u_0 > E + mc^2, \tag{12}$$

since in this case the paradox arises. The wave vector q is real and we have a propagating wave on the right side of the barrier. Note, however, that this particle belongs to the hole continuum rather than to the electron one. For smaller values of u_0, there are either propagating electrons on both the left and the right side of the barrier, when $u_0 < E - mc^2$, or evanescent waves on the right side of the barrier, when $E - mc^2 < u_0 < E + mc^2$. Solving the Dirac equation (3) on the right side of the barrier, one obtains for the transmitted wave

$$\Psi_t(x) = \begin{pmatrix} 1 \\ -1/\beta \end{pmatrix} {\rm e}^{{\rm i}qx}, \tag{13}$$

where

$$\beta = \sqrt{\frac{u_0 - E - mc^2}{u_0 - E + mc^2}}. \tag{14}$$

From the continuity of the wavefunction at $x = 0$,

$$\Psi_{\rm in} + r\Psi_{\rm r}|_{x=-0} = \Psi_t|_{x=+0}, \tag{15}$$

we find

$$r = \frac{\alpha\beta + 1}{\alpha\beta - 1}. \tag{16}$$

For the considered case, we have $0 < \alpha, \beta < 1$, so that $r < 0$ and

$$R = |r|^2 = \left(\frac{1 + \alpha\beta}{1 - \alpha\beta}\right)^2 > 1. \tag{17}$$

To treat reflection and transmission coefficients properly, one has to look at the probability current density for the 1D Dirac equation

$$j_x = c\Psi^\dagger\sigma_x\Psi = c(\psi_1^*\psi_2 + \psi_2^*\psi_1), \tag{18}$$

which is a conserved quantity. When we look at the current density (18) we see that it takes the values $2\alpha c$ for the incoming wave and $-2\alpha cR$ for the reflected wave. Therefore R is nothing but the reflection coefficient and we come to the conclusion that the amplitude of the reflected wave is larger than that of the incident wave. This strange effect that occurs when condition (12) is fulfilled was initially called the Klein paradox. In the following discussion, we will follow [10] and [11]. For a rather complete list of references, see [12].

First of all, note that the current density (18) on the right-hand side is equal to $-2|t|^2/\beta$, indicating that there is something wrong with the definition of the transmitted wave. What exactly is wrong has been pointed out by Pauli, who noticed that the group velocity for the case of equation (12),

$$v_{\rm g} = \frac{1}{\hbar}\frac{{\rm d}E}{{\rm d}q} = \frac{1}{\hbar}\left(\frac{{\rm d}q}{{\rm d}E}\right)^{-1} = \frac{\hbar c^2 q}{E - u_0} \tag{19}$$

is opposite to the direction of the wave vector q. Since the group velocity determines the direction of propagation, the transmitted wave (13) corresponds (for positive q) to a particle moving to the left instead of to the right. Therefore, we should define our outgoing wave as

$$\Psi_t(x) = \begin{pmatrix} 1 \\ 1/\beta \end{pmatrix} {\rm e}^{-{\rm i}qx}, \tag{20}$$

which gives the current density $2|t|^2/\beta$. When we once again calculate r from equation (15), it is seen that

$$R = |r|^2 = \left(\frac{1 - \alpha\beta}{1 + \alpha\beta}\right)^2 < 1. \tag{21}$$

which is always smaller than 1. Therefore the formal paradox disappears; see also [13].

The paradox reappears when we consider the problem from a different angle. Instead of an infinitely broad barrier, we will consider a finite barrier,

$$u(x) = \begin{cases} u_0, & |x| < a, \\ 0, & |x| > a. \end{cases} \tag{22}$$

The problem with the choice of the transmitted wave on the right side of the barrier has now disappeared, since it is simply $t\Psi_{\text{in}}$. Within the barrier, one now has to consider both modes $\exp(\pm iqx)$, representing the most general solution. Reflection and transmission coefficients are then obtained from the continuity of the wavefunction at $x = -a$ and $x = a$, which gives after straightforward calculations (see e.g. [10] and [14])

$$R = \frac{(1-\alpha^2\beta^2)^2 \sin^2(2qa)}{4\alpha^2\beta^2 + (1-\alpha^2\beta^2)^2 \sin^2(2qa)}, \tag{23}$$

$$T = \frac{4\alpha^2\beta^2}{4\alpha^2\beta^2 + (1-\alpha^2\beta^2)^2 \sin^2(2qa)}. \tag{24}$$

There is no paradox in these expressions, since $0 < R < 1$, $0 < T < 1$ and $R + T = 1$ as it should be. Note that we have total transmission through the barrier when

$$qa = \frac{N\pi}{2}, \tag{25}$$

with integer N.

We can consider an infinitely broad barrier by letting a go to infinity in the above expressions. As a becomes very large, while other parameters remain fixed, the sine will oscillate very rapidly. We can then average over the fast oscillations and replace $\sin^2(2qa)$ by its average value $\frac{1}{2}$ to obtain the expressions

$$R_\infty = \frac{(1-\alpha^2\beta^2)^2}{8\alpha^2\beta^2 + (1-\alpha^2\beta^2)^2}, \tag{26}$$

$$T_\infty = \frac{8\alpha^2\beta^2}{8\alpha^2\beta^2 + (1-\alpha^2\beta^2)^2}. \tag{27}$$

One may be surprised that the results (21) and (26) do not coincide. It is, however, well known from electromagnetic wave theory [15] that the reflection coefficients for the two situations should differ.

From the last result we see once again that the paradox has disappeared in its mathematical form, but has reappeared as physically counterintuitive behavior. In non-relativistic quantum mechanics a particle can tunnel through a classically forbidden region $E < u(x)$, but the probability is exponentially small when the barrier is high and broad. In the semiclassical approximation, the transmission through the barrier with turning points $x_{1,2}$, which satisfy $E = u(x_{1,2})$, is given by

$$T = \exp\left(-\frac{2}{\hbar}\int_{x_1}^{x_2} \mathrm{d}x\sqrt{2m(u(x)-E)}\right), \tag{28}$$

where m is the mass of the particle. For a relativistic particle incident on a sufficiently high barrier (12), the situation is dramatically different. In the limit $a \to \infty$, the probability of penetration (27) is, in general, not small at all. Even for an infinitely high barrier ($u_0 \to \infty$), one has $\beta = 1$ and

$$T_\infty = \frac{E^2 - m^2c^4}{E^2 - \frac{1}{2}m^2c^4}. \tag{29}$$

This is of the order of 1 when $E - mc^2$ is of the order of mc^2, while it is approximately equal to 1 in the ultrarelativistic limit

$$E \gg mc^2. \tag{30}$$

This is the contemporary formulation of the Klein paradox [10]; quantum relativistic particles can tunnel with large enough probabilities through barriers of arbitrarily large height and width.

The tunneling effect can be hand-wavingly explained with the help of the Heisenberg uncertainty principle. Since one cannot know both momentum and position with an arbitrary accuracy at a given instant, one cannot separate the total energy into a potential and a kinetic part. Hence, the kinetic energy can be 'a bit' negative. In the relativistic regime, the restriction is much stronger [16]: one cannot even know the coordinate with an accuracy higher than $\hbar c/E$. Therefore relativistic quantum mechanics cannot be mechanics, but can only be field theory [17]. This theory will always contain particles and antiparticles and to measure the coordinate better than $\hbar c/E$, one needs to apply such a high energy that particle–antiparticle pairs will be created. The original particle whose coordinate one wanted to measure will then be lost among the newly born particles. A full field theoretic treatment of the problem is given in [18]. The most important point is that although the problem of a high enough barrier looks like a static problem, this is actually not the case. One needs to study carefully how the state is reached and this involves positron emission by the growing barrier. For a more detailed discussion of the role of electron–positron pairs in the Klein paradox, see [19].

3. Klein tunneling in single-layer graphene

The Hamiltonian for charge carriers in graphene near conical points K and K' is given by the massless Dirac Hamiltonian

$$\hat{H} = V(\sigma_x \hat{p}_x + \sigma_y \hat{p}_y) + u(x, y), \tag{31}$$

where V is the Fermi velocity $V \approx c/300$. To consider normal incidence on the 1D potential barrier (22) in this case, we can simply put $m = 0$ in our previous results. From equations (10) and (14) it is seen that $\alpha = \beta = 1$. Therefore we have $T = 1$ and $R = 0$ in equations (26) and (27), regardless of the height of the potential. This result is not related to the specific shape of the potential [20].

This property has an analogue in 2D and 3D with $u = u(x, y)$ or $u = u(x, y, z)$, namely that backscattering is forbidden. This was found long ago for scattering of ultrarelativistic particles in 3D (see [17, 21]). An important consequence of this property for carbon materials was noted in [20]. Absence of backscattering explains the existence of conducting channels in metallic carbon nanotubes, while in a non-relativistic 1D system an arbitrarily small disorder leads to localization [22].

The consideration in [20] is very instructive since it explicitly shows the role of the Berry phase and time-reversal symmetry, but it is quite cumbersome. Here we present a somewhat simplified scheme of this proof. To this aim we consider the equation for the T-matrix (see e.g. [23])

$$\hat{T} = \hat{u} + \hat{u}\hat{G}_0\hat{T}, \tag{32}$$

where $\hat{u}$ is the operator corresponding to the scattering potential,

$$\hat{G}_0 = \lim_{\delta\to+0} \frac{1}{E - \hat{H}_0 + \mathrm{i}\delta} \tag{33}$$

is the Green's function of the unperturbed Hamiltonian $\hat{H}_0$ and E is the electron energy, which is assumed to be larger than zero. If $\hat{H}_0$ is the Dirac Hamiltonian for massless Dirac fermions (31), we have

$$\hat{G}_0(\mathbf{r}, \mathbf{r}') = \int \frac{\mathrm{d}\mathbf{q}}{(2\pi)^2} \hat{G}_0(\mathbf{q}) \exp[\mathrm{i}\mathbf{q}(\mathbf{r} - \mathbf{r}')] \,, \tag{34}$$

where

$$\hat{G}_0(\mathbf{q}) = \frac{1}{E - \hbar V \mathbf{q}\boldsymbol{\sigma} + \mathrm{i}\delta} = \frac{1}{\hbar V} \frac{\varepsilon + \mathbf{q}\boldsymbol{\sigma}}{(\varepsilon + \mathrm{i}\delta)^2 - q^2}, \tag{35}$$

with $\varepsilon = E/\hbar V$. The probability of backscattering can be found by iterating equation (32) and is proportional to

$$\begin{aligned} T(-\mathbf{k}, \mathbf{k}) &= \langle -\mathbf{k}|u + u\hat{G}_0 u + u\hat{G}_0 u\hat{G}_0 u + \cdots |\mathbf{k}\rangle \\ &\equiv T^{(1)} + T^{(2)} + \cdots, \end{aligned} \tag{36}$$

where $T^{(n)}$ is the contribution proportional to u^n.

We can always choose the axes such that $\mathbf{k} \| Ox$. In this case, $|\mathbf{k}\rangle$ and $|-\mathbf{k}\rangle$ have spinor structures $\binom{1}{1}$ and $\binom{1}{-1}$, respectively. Therefore, if $\hat{T}$ is the 2×2 matrix

$$\hat{T} = T_0 + \boldsymbol{T}\boldsymbol{\sigma}, \tag{37}$$

one has

$$T(-\mathbf{k}, \mathbf{k}) \sim T_z(-\mathbf{k}, \mathbf{k}) + \mathrm{i}T_y(-\mathbf{k}, \mathbf{k}). \tag{38}$$

Now keeping in mind that V is proportional to the identity matrix, one can prove term by term that all contributions to $T_y(-\mathbf{k}, \mathbf{k})$ and $T_z(-\mathbf{k}, \mathbf{k})$ vanish by symmetry. Actually this is because $\hat{\mathbf{T}}(\mathbf{k}) \sim \mathbf{k} \,\|Ox$; from the vectors $\mathbf{k}$ and $-\mathbf{k}$ one cannot construct anything with non-zero y or z components. Strictly speaking this argument is only valid for an isotropic potential; for a generic case, one has to do a term-by-term analysis based on expansion (36); see [20]. For two nonparallel vectors $\mathbf{k_1}$ and $\mathbf{k_2}$ one can construct a matrix with nonzero y- or z-components, since one of the vectors has a non-zero y-component, so that $\mathbf{k_1} \times \mathbf{k_2} \| Oz$.

When one thinks of electrons in quantum electrodynamics, it is not easy to create potential jumps larger than $2mc^2 \approx 1\,\mathrm{MeV}$. Similar phenomena take place in electric or gravitational fields ([24, 25]; see [12] for a detailed list of references), but the context is always quite exotic, such as collisions of ultraheavy ions or even black hole evaporation. There were no experimental data available that would require the Klein paradox for their explanation. However, shortly after the discovery of graphene it was realized that Klein tunneling is one of the crucial phenomena for graphene physics and electronics [8]. Soon after this theoretical prediction the effect was confirmed experimentally [26, 27].

Considering possible applications, Klein tunneling in graphene is rather bad news. If one copied the construction from a silicon transistor to graphene, it would be impossible to lock the transistor. One would need to open a gap in the spectrum to be able to lock it. At the same time, it is good news as well: due to the Klein paradox, inhomogeneities in the electron density do not lead to localization and their effect on the electron mobility is not essential [8].

4. Tunneling through a stepwise barrier

Let us now consider a massless Dirac fermion incident on the potential barrier (22) with positive energy under an angle ϕ, as was first done in [8]. Of course, the potential cannot be sharp on the atomic scale, since this would induce Umklapp scattering between different valleys. Therefore, by a stepwise potential, we mean that the electron wavelength k^{-1} is much larger than the typical spatial scale of the potential l, which, in turn, is much larger than the size of the unit cell.

Within this assumption the solution in each region is given by traveling waves proportional to $\exp(\pm\mathrm{i}k_x x)$ $\exp(\pm\mathrm{i}k_y y)$, where k_x and k_y satisfy the dispersion relation

$$\left(\frac{E - u_0}{\hbar V}\right)^2 \equiv k^2 = (k_x^2 + k_y^2), \tag{39}$$

as can be found from equation (31). Similarly to the original Dirac equation, we can distinguish three distinct regimes from this equation. For $u_0 < E - \hbar V|k_y|$ we have electrons and for $u_0 > E + \hbar V|k_y|$ we have holes, while the region $E - \hbar V|k_y| < u_0 < E + \hbar V|k_y|$ is classically forbidden. As was done for the case of the massive Dirac equation, we will now require that the potential u_0 in equation (22) satisfies

$$u_0 > E + \hbar V|k_y|, \tag{40}$$

so that we have hole states within the barrier.

Let us denote by k the wave vector for $|x| > a$ and by q the wave vector for $|x| < a$. At the potential jump the momentum in the y-direction should be conserved, so that the new angle θ is related to the new wave vector q by

$$k \sin\phi = k_y = q_y = q \sin\theta. \tag{41}$$

From equation (31), we can see that the second component of the wavefunction is related to the first one by

$$\psi_2 = \mathrm{sgn}(E - u_0)\mathrm{e}^{\mathrm{i}\phi}\psi_1, \tag{42}$$

so the solutions in the three regions are given by

$$\Psi(x, y) = \begin{cases} \begin{pmatrix} 1 \\ s\,\mathrm{e}^{\mathrm{i}\phi} \end{pmatrix} \mathrm{e}^{\mathrm{i}k_x x}\,\mathrm{e}^{\mathrm{i}k_y y} + r \begin{pmatrix} 1 \\ -s\,\mathrm{e}^{-\mathrm{i}\phi} \end{pmatrix} \mathrm{e}^{-\mathrm{i}k_x x}\,\mathrm{e}^{\mathrm{i}k_y y}, & x < -a, \\ A \begin{pmatrix} 1 \\ s'\,\mathrm{e}^{\mathrm{i}\theta} \end{pmatrix} \mathrm{e}^{\mathrm{i}q_x x}\,\mathrm{e}^{\mathrm{i}k_y y} + B \begin{pmatrix} 1 \\ -s'\,\mathrm{e}^{-\mathrm{i}\theta} \end{pmatrix} \mathrm{e}^{-\mathrm{i}q_x x}\,\mathrm{e}^{\mathrm{i}k_y y}, & -a < x < a, \\ t \begin{pmatrix} 1 \\ s\,\mathrm{e}^{\mathrm{i}\phi} \end{pmatrix} \mathrm{e}^{\mathrm{i}k_x x}\,\mathrm{e}^{\mathrm{i}k_y y}, & x > a, \end{cases} \tag{43}$$

where we have introduced $s = \mathrm{sgn}(E)$, $s' = \mathrm{sgn}(E - u_0)$, $k_x = k\cos\phi$ and $q_x = q\cos\theta$. Note that the reflected particle moves under the angle $\pi - \phi$, assuming that the angle changes from $-\pi/2$ to $3\pi/2$, so that we have the phase $-\exp(-\mathrm{i}\phi)$ for the reflected wave. We can now determine the reflection coefficient r, the transmission coefficient t and the coefficients A and B as before, from the requirement that the wavefunction is continuous at $x = \pm a$.

Finally, the result is given by

$$r = 2\,\mathrm{e}^{\mathrm{i}\phi - 2\mathrm{i}k_x a}\sin(2q_x a) \times \frac{\sin\phi - ss'\sin\theta}{ss'\left[\mathrm{e}^{-2\mathrm{i}q_x a}\cos(\phi+\theta) + \mathrm{e}^{2\mathrm{i}q_x a}\cos(\phi-\theta)\right] - 2\mathrm{i}\sin(2q_x a)}. \tag{44}$$

For the case under consideration, we have $ss' = -1$, since the signs of E and $E - u_0$ are opposite. The transmission probability can now be easily calculated as

$$T = |t|^2 = 1 - |r|^2. \tag{45}$$

From equation (44), we immediately see that the reflection is zero for normal incidence, as we proved for a more general potential in the previous section. There are also additional angles, called 'magic angles', at which the reflection coefficient is zero and we have full transmission. They are given by the condition

$$q_x a = N\frac{\pi}{2}, \tag{46}$$

where N is an integer.

We can compare the behavior of electrons in single-layer graphene with the behavior of normal electrons. When the potential barrier contains no electronic states, the transmission decays exponentially with increasing barrier width and height [28], so that the barrier would reflect electrons completely. But since single-layer graphene is gapless, it seems more appropriate to compare it to a gapless semiconductor with non-chiral charge carriers, a situation that can be realized in certain heterostructures [29, 30]. For this case, we find that

$$t = \frac{4k_x q_x \exp(2\mathrm{i}q_x a)}{(q + k_x)^2\exp(-2\mathrm{i}q_x a) - (q_x - k_x)^2\exp(2\mathrm{i}q_x a)}, \tag{47}$$

where k_x and q_x are the x-components of the wave vector outside and inside the barrier, respectively. As in the case of single-layer graphene, there are resonance conditions at which the barrier is transparent, given by $2q_x a = N\pi$, where N is an integer. For normal incidence, we see that the transmission coefficient is an oscillating function of the tunneling parameters and can exhibit any value between zero and one. This is in contrast with single-layer graphene, where the transmission is always perfect.

5. Klein tunneling in bilayer graphene

Bilayer graphene consists of two layers of graphene one on top of the other, the second layer being rotated by 120° with respect to the first one. In this configuration, the sublattices A lie exactly on top of each other and the hopping parameter γ_1 between them is approximately 0.4 eV [31, 32], while the in-plane hopping parameter $\gamma_0 = t$ is approximately an order of magnitude larger. When we consider only low-energy excitations, $|E|, |E - u_0| \ll 2|\gamma_1|$, the effective Hamiltonian is given by [33, 34]

$$\hat{H} = \begin{pmatrix} 0 & (\hat{p}_x - \mathrm{i}\hat{p}_y)^2/(2m) \\ (\hat{p}_x + \mathrm{i}\hat{p}_y)^2/(2m) & 0 \end{pmatrix} + u(x), \tag{48}$$

where the effective mass $m = \gamma_1/2V^2 \approx 0.054 m_\mathrm{e}$, with m_e being the free electron mass [35]. There is also hopping between the B sublattices of both layers, which is denoted by $\gamma_3 \approx 0.3$ eV. When we include this parameter in the description, an extra term is added to the Hamiltonian, which corresponds to the so-called trigonal warping. This effect is, however, only important for small wave vectors [35]; we will exclude it assuming that $ka, qa \gg \gamma_3\gamma_1/\gamma_0^2$.

Let us consider an electron incident on the potential step (22) under an angle ϕ, as was done in [8]. Since the potential is constant in the y-direction, we can write the solution as

$$\Psi(x, y) = \Psi(x)\mathrm{e}^{\mathrm{i}k_y y}. \tag{49}$$

Inserting this into equation (1) with the Hamiltonian (48), we obtain

$$\left(\frac{\mathrm{d}^2}{\mathrm{d}x^2} - k_y^2\right)^2 \psi_i = \left(\frac{2m(E-u)}{\hbar^2}\right)^2 \psi_i \equiv k^4\psi_i. \tag{50}$$

The solutions are therefore given by propagating waves $\exp(\pm\mathrm{i}k_x x)$ and exponentially growing and decaying modes $\exp(\pm\kappa_x x)$,

$$k_x^2 + k_y^2 = \frac{2m|E-u|}{\hbar^2}, \tag{51}$$

$$\kappa_x^2 - k_y^2 = \frac{2m|E-u|}{\hbar^2}. \tag{52}$$

The presence of evanescent modes is markedly different from both the Schrödinger case and the Dirac case. Once again there are three regimes. There are electron states for $u_0 < E - \hbar^2 k_y^2/(2m)$ and hole states for $u_0 > E + \hbar^2 k_y^2/(2m)$, while the region in between is classically forbidden. In what follows, we assume that u_0 in equation (22) satisfies

$$u_0 > E + \frac{\hbar^2 k_y^2}{2m}. \tag{53}$$

To find the spinors that are the solutions to equation (50), we note that the components are related by

$$\left(\frac{\mathrm{d}}{\mathrm{d}x} + k_y\right)^2 \psi_2 = \frac{2m(E-u)}{\hbar^2}\psi_1, \tag{54}$$

as can be seen from the Hamiltonian (48).

Now let $k = \sqrt{2mE}/\hbar$ be the wave vector for the propagating modes in the region $|x| > a$, while $q = \sqrt{2m(u_0 - E)}/\hbar$ is the wave vector in the region $|x| < a$. Then the solution for $x < -a$ is given by

$$\Psi(x) = a_1\begin{pmatrix}1\\ s\,\mathrm{e}^{2\mathrm{i}\phi}\end{pmatrix}\mathrm{e}^{\mathrm{i}k_x x} + b_1\begin{pmatrix}1\\ s\,\mathrm{e}^{-2\mathrm{i}\phi}\end{pmatrix}\mathrm{e}^{-\mathrm{i}k_x x} + c_1\begin{pmatrix}1\\ -sh_1\end{pmatrix}\mathrm{e}^{\kappa_x x}, \tag{55}$$

where $k_y = k\sin\phi$, $k_x = k\cos\phi$, $s = \mathrm{sgn}(E)$, $\kappa_x = \sqrt{k_x^2 + 2k_y^2} = k\sqrt{1+\sin^2\phi}$ and finally $h_1 = (\sqrt{1+\sin^2\phi} - \sin\phi)^2$. The amplitude a_1 is the amplitude for the incoming wave in this expression, while b_1 corresponds to the reflected wave. For $x > a$, we have the general solution

$$\Psi(x) = a_3 \begin{pmatrix} 1 \\ s\,\mathrm{e}^{2\mathrm{i}\phi} \end{pmatrix} \mathrm{e}^{\mathrm{i}k_x x} + d_3 \begin{pmatrix} 1 \\ -s/h_1 \end{pmatrix} \mathrm{e}^{-\kappa_x x}, \tag{56}$$

where a_3 is the transmission coefficient. Inside the barrier we need the most general solution with two propagating modes and two modes with real exponentials,

$$\Psi(x) = a_2 \begin{pmatrix} 1 \\ s'\,\mathrm{e}^{2\mathrm{i}\theta} \end{pmatrix} \mathrm{e}^{\mathrm{i}q_x x} + b_2 \begin{pmatrix} 1 \\ s'\,\mathrm{e}^{-2\mathrm{i}\theta} \end{pmatrix} \mathrm{e}^{-\mathrm{i}q_x x} + c_2 \begin{pmatrix} 1 \\ -s'h_2 \end{pmatrix} \mathrm{e}^{\lambda_x x} + d_2 \begin{pmatrix} 1 \\ -s'/h_2 \end{pmatrix} \mathrm{e}^{-\lambda_x x}, \tag{57}$$

where $q_y = q\sin\theta = k_y$ because the transverse momentum is conserved. Furthermore, $q_x = q\cos\theta$, $s' = \mathrm{sgn}(E - u_0)$, $\lambda_x = q\sqrt{1+\sin^2\theta}$ and $h_2 = (\sqrt{1+\sin^2\theta} - \sin\theta)^2$.

Now the coefficients a_i, b_i, c_i and d_i have to be found from the continuity of $\psi_i(x)$ and the derivative $\mathrm{d}\psi_i/\mathrm{d}x$ at the points $x = \pm a$. When the problem is solved numerically, one sees that the transmission probability at normal incidence is exponentially small. Similar to the case of single-layer graphene, there are once again 'magic angles' in the spectrum, at which there is total transmission. The existence of magic angles in bilayer graphene has the same consequences as in single-layer graphene, meaning that we cannot lock a conventional transistor made of bilayer graphene.

For the case of normal incidence $\phi = \theta = 0$, we can also solve the problem analytically. The transmission coefficient is given by

$$t = \frac{4\mathrm{i}kq\exp(2\mathrm{i}ka)}{(q+\mathrm{i}k)^2\exp(-2qa) - (q-\mathrm{i}k)^2\exp(2qa)}, \tag{58}$$

which is indeed exponentially small. When we let a go to infinity, the transmission probability $T = |t|^2$ becomes zero at normal incidence. Furthermore, for a single n–p junction with $u_0 \gg E$, the following analytical solution can be found for any ϕ:

$$T = \frac{E}{u_0}\sin^2(2\phi), \tag{59}$$

which also gives $T = 0$ at normal incidence, in contrast with the case of single-layer graphene, where normally incident electrons are always transmitted. It is also different from the case of normal electrons, where the transmission is given by equation (47).

6. Dimensionless variables and parameters

In sections 3 and 5, it was mentioned that the wavefunctions Ψ of charge carriers in single-layer and bilayer graphene in 1D geometry obey the equations

$$\left[V\begin{pmatrix} 0 & \hat{p}_x - \mathrm{i}p_y \\ \hat{p}_x + \mathrm{i}p_y & 0 \end{pmatrix} + u(x/l) - E\right]\Psi = 0 \tag{60}$$

and

$$\left[\frac{1}{2m}\begin{pmatrix} 0 & (\hat{p}_x - \mathrm{i}p_y)^2 \\ (\hat{p}_x + \mathrm{i}p_y)^2 & 0 \end{pmatrix} + u(x/l) - E\right]\Psi = 0, \tag{61}$$

respectively. Here l is a characteristic scale of a potential change. In dimensionless variables, (60) takes the form

$$\left[\begin{pmatrix} 0 & \tilde{p}_x - \mathrm{i}\tilde{p}_y \\ \tilde{p}_x + \mathrm{i}\tilde{p}_y & 0 \end{pmatrix} + \tilde{u}(\tilde{x}) - \widetilde{E}\right]\Psi = 0, \tag{62}$$

where $\tilde{x} = x/l$, $\tilde{p}_x = -\mathrm{i}h\,\mathrm{d}/\mathrm{d}\tilde{x}$, $\tilde{p}_y = p_y/p_0$, $h = \hbar/p_0 l$, $\tilde{u} = u/Vp_0$ and $\widetilde{E} = E/Vp_0$. We denote some characteristic value of $|u - E|$ as Vp_0.

Analogously, (61) can be rewritten as

$$\left[\begin{pmatrix} 0 & (\tilde{p}_x - \mathrm{i}\tilde{p}_y)^2 \\ (\tilde{p}_x + \mathrm{i}\tilde{p}_y)^2 & 0 \end{pmatrix} + \tilde{u}(\tilde{x}) - \widetilde{E}\right]\Psi = 0, \tag{63}$$

with $\tilde{x} = x/l$, $\tilde{p}_x = -\mathrm{i}h\,\mathrm{d}/\mathrm{d}\tilde{x}$, $\tilde{p}_y = p_y/p_0$, $h = \hbar/p_0 l$, $\tilde{u} = 2mu/p_0^2$ and $\widetilde{E} = 2mE/p_0^2$. We denote some characteristic value of $|u - E|$ as $p_0^2/2m$.

Thus, we can introduce dimensionless Hamiltonians (we omitted tildes):

$$\hat{H} = \begin{pmatrix} 0 & \hat{p}_x - \mathrm{i}p_y \\ \hat{p}_x + \mathrm{i}p_y & 0 \end{pmatrix} + u(x) \tag{64}$$

for a single layer and

$$\hat{H} = \begin{pmatrix} 0 & (\hat{p}_x - \mathrm{i}p_y)^2 \\ (\hat{p}_x + \mathrm{i}p_y)^2 & 0 \end{pmatrix} + u(x) \tag{65}$$

for a bilayer. In both cases, there are two substantial parameters in the problem: h and p_y.

7. Standard semiclassical treatment

Charge carriers in single-layer graphene are described by the Hamiltonian (64). This Hamiltonian describes simultaneously coupled electron and hole states. According to appendix A, in the adiabatic approximation, (64) can be diagonalized up to any order of $h \ll 1$. The obtained scalar Hamiltonians describe electrons and holes separately. The diagonalization is based on a series of unitary transformations of the original Hamiltonian and traces back to the ideas of the Foldy–Wouthuysen transformation [36] and the Peierls substitution in Blount's treatment [37]. We use its variant [38, 39].

Effective electron and hole Hamiltonians $\hat{L}^+$ and $\hat{L}^-$can be written as series with respect to the small parameter h:

$$L^{\pm}(\hat{p}_x, x, h) = L_0^{\pm}(\hat{p}_x, x) + hL_1^{\pm}(\hat{p}_x, x) + h^2 L_2^{\pm}(\hat{p}_x, x) + \cdots. \tag{66}$$

To be precise we will assume that any function of $\hat{p}_x$ and x is defined in such a way that $\hat{p}_x$acts first. As soon as the ordering of operators has been introduced, one can work with functions of c-numbers p_x and x. These functions are called 'symbols' [40, 41].

It is shown in appendix A that leading terms $L_0^{\pm}(p_x, x)$ of the effective Hamiltonians $L^{\pm}(p_x, x, h)$ are eigenvalues of $H(p_x, x)$:

$$H(p_x, x)\chi_0^{\pm}(p_x, x) = L_0^{\pm}(p_x, x)\chi_0^{\pm}(p_x, x), \tag{67}$$

where $\chi_0^\pm(p_x,x)$ are two eigenvectors of the matrix $H(p_x,x)$. This gives

$$L_0^\pm(p_x,x)=\pm|p|+u(x),\quad \chi_0^\pm(p_x)=\frac{1}{\sqrt{2}}\begin{pmatrix}\mathrm{e}^{-\mathrm{i}\phi_p}\\ \pm 1\end{pmatrix}. \tag{68}$$

We note that in the absence of a magnetic field, $\chi_0^\pm$ does not depend on x. The first correction $L_1^\pm(p_x,x)$ reads

$$\begin{aligned}L_1^\pm(p_x,x)&=\mathrm{i}\left(\chi_0^\pm\right)^\dagger\frac{\partial\chi_0^\pm}{\partial p_x}\frac{\partial L_0^\pm}{\partial x}=\frac{1}{2}\frac{\partial L_0^\pm}{\partial x}\frac{\partial\phi_p}{\partial p_x}\\&=-\frac{u'(x)}{2}\frac{p_y}{p_x^2+p_y^2}.\end{aligned} \tag{69}$$

A standard semiclassical treatment (see appendix B) can be applied to scalar Schrödinger-like equations $\hat{L}^\pm\psi^\pm=E\psi^\pm$. We are looking for a solution of the form $\psi^\pm=\mathrm{e}^{\mathrm{i}S^\pm(x)/h}A^\pm(x,h)$, $A^\pm(x,h)=A_0^\pm(x)+hA_1^\pm(x)+\cdots$ This gives

$$\begin{aligned}A_0^\pm(x)=&\left|\frac{\partial L_0^\pm}{\partial p_x}\right|^{-1/2}\\&\times\exp\left[-\mathrm{i}\int\mathrm{d}x\left(\frac{\partial L_0^\pm}{\partial p_x}\right)^{-1}\left(L_1^\pm+\frac{\mathrm{i}}{2}\frac{\partial^2 L_0^\pm}{\partial p_x\partial x}\right)\right]\end{aligned} \tag{70}$$

with $p_x=\mathrm{d}S^\pm/\mathrm{d}x$ to be found from the Hamilton–Jacobi equation $L_0^\pm(p_x,x)=E$, where

$$\left|\frac{\partial L_0^\pm}{\partial p_x}\right|=\frac{|p_x|}{|p|}=\frac{\left([E-u(x)]^2-p_y^2\right)^{1/2}}{|E-u(x)|}. \tag{71}$$

Differentiating the Hamilton–Jacobi equation with respect to x, we find that

$$\frac{\partial L_0^\pm}{\partial p_x}\frac{\mathrm{d}p_x}{\mathrm{d}x}+\frac{\partial L_0^\pm}{\partial x}=0, \tag{72}$$

when

$$\frac{\partial L_0^\pm}{\partial p_x}=-\frac{1}{p_x'}\frac{\partial L_0^\pm}{\partial x}. \tag{73}$$

This gives

$$\psi(x)=\frac{|E-u(x)|^{1/2}}{\left[(E-u(x))^2-p_y^2\right]^{1/4}}\mathrm{e}^{\pm\mathrm{i}S^+(x)/h+\mathrm{i}\phi_p^\pm(x)/2}. \tag{74}$$

Although it is possible to define locally $\chi_0^\pm$ in (68) as

$$\chi_0^\pm(p_x)=\frac{1}{\sqrt{2}}\begin{pmatrix}\mathrm{e}^{-\mathrm{i}\phi_p/2}\\ \pm\mathrm{e}^{\mathrm{i}\phi_p/2}\end{pmatrix} \tag{75}$$

to obtain $L_1^\pm=0$, such a choice does not provide a single-valued function in the classical phase space.

Let us first consider a scattering problem for $p_y\neq 0$ following appendices B and C. For an electron coming from the left of the classically forbidden region, we have

$$\begin{aligned}\psi(x)=&\frac{|E-u(x)|^{1/2}}{\left[(E-u(x))^2-p_y^2\right]^{1/4}}\\&\times\left(\mathrm{e}^{\mathrm{i}S^+(x)/h+\mathrm{i}\phi_p^+(x)/2}+\mathrm{e}^{-\mathrm{i}S^+(x)/h+\mathrm{i}\phi_p^-(x)/2-\mathrm{i}\pi/2}\right)\end{aligned} \tag{76}$$

and

$$\begin{aligned}\Psi(x)=&\frac{|E-u(x)|^{1/2}}{\left[(E-u(x))^2-p_y^2\right]^{1/4}}\\&\times\begin{pmatrix}\mathrm{e}^{\mathrm{i}S^+(x)/h-\mathrm{i}\phi_p^+(x)/2}+\mathrm{e}^{-\mathrm{i}S^+(x)/h-\mathrm{i}\phi_p^-(x)/2-\mathrm{i}\pi/2}\\ \mathrm{e}^{\mathrm{i}S^+(x)/h+\mathrm{i}\phi_p^+(x)/2}+\mathrm{e}^{-\mathrm{i}S^+(x)/h+\mathrm{i}\phi_p^-(x)/2-\mathrm{i}\pi/2}\end{pmatrix},\end{aligned} \tag{77}$$

where

$$\begin{aligned}S^\pm(x)&=\pm\int_{x_0}^x\sqrt{v^2(x')-p_y^2}\,\mathrm{d}x',\\ \phi_p^\pm(x)&=\arg\left(\pm\sqrt{v^2(x)-p_y^2}+\mathrm{i}p_y\right),\end{aligned} \tag{78}$$

$$\phi_p^-(x)=\pi\,\mathrm{sgn}(p_y)-\phi_p^+(x),\quad v(x)=u(x)-E. \tag{79}$$

Note that $\phi_p^+(x)$ continuously depends on p_y when it passes through zero and $\phi_p^-(x)$ undergoes a jump of 2π. The reflection coefficient r can be computed from (76) or (77) as the coefficient in front of the semiclassical solution corresponding to the outgoing wave. One can also assume that the potential tends to a constant at infinity and take the coefficient in front of the plane wave, which is a particular case of the definition given above. Obviously, the reflection coefficient defined in such a way does not depend on x. Choosing (74) as incoming and outgoing solutions, we can write wavefunctions on the left of the classically forbidden region as

$$\begin{aligned}\psi(x)=&\frac{|E-u(x)|^{1/2}}{\left[(E-u(x))^2-p_y^2\right]^{1/4}}\\&\times(\mathrm{e}^{\mathrm{i}S^+(x)/h+\mathrm{i}\phi_p^+(x)/2}+r(p_y)\mathrm{e}^{-\mathrm{i}S^+(x)/h+\mathrm{i}\phi_p^-(x)/2}),\end{aligned} \tag{80}$$

$$\begin{aligned}\Psi(x)=&\frac{|E-u(x)|^{1/2}}{\left[(E-u(x))^2-p_y^2\right]^{1/4}}\\&\times\left[\begin{pmatrix}\mathrm{e}^{\mathrm{i}S^+(x)/h-\mathrm{i}\phi_p^+(x)/2}\\ \mathrm{e}^{\mathrm{i}S^+(x)/h+\mathrm{i}\phi_p^+(x)/2}\end{pmatrix}\right.\\&\left.+r(p_y)\begin{pmatrix}\mathrm{e}^{-\mathrm{i}S^+(x)/h-\mathrm{i}\phi_p^-(x)/2}\\ \mathrm{e}^{-\mathrm{i}S^+(x)/h+\mathrm{i}\phi_p^-(x)/2}\end{pmatrix}\right],\end{aligned} \tag{81}$$

Comparing (80), (81) and (76), (77), we conclude that

$$r(p_y)=\mathrm{e}^{-\mathrm{i}\pi/2}. \tag{82}$$

A similar calculation for a hole coming from the right gives, see also figure 1,

$$r(p_y)=\mathrm{e}^{\mathrm{i}\pi/2}. \tag{83}$$

We paid attention to the definition of the reflection coefficient, since it may lead to a discrepancy for the Dirac particle. The problem appears due to a jump of 2π in $\phi_p^-(x)$ at any fixed x as a function of p_y when it goes through zero. This jump is a consequence of the cut at $\phi_p=\pm\pi$. At any $p_y\neq 0$, this cut corresponds to an infinite negative x-component of the momentum, and does not imply any discontinuities in the

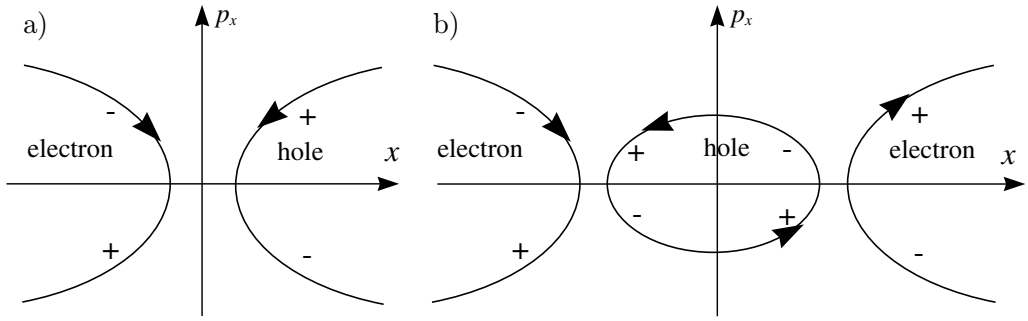

Figure 1. Classical phase space for (a) n–p and (b) n–p–n junctions. In the electronic region, the velocity is codirectional with the momentum, and in the hole region, the velocity is in the opposite direction to the momentum. Therefore electronic trajectories are oriented clockwise, but hole trajectories are oriented counterclockwise. Plus and minus signs denote signs of $\mathrm{d}p_x/\mathrm{d}x$.

region where the potential is finite. This jump results in the jump of π in the phase of the wavefunction corresponding to the outgoing wave. However, the phase difference $\phi_p^-(x)/2 - \phi_p^+(x)/2 = \pi\ \mathrm{sgn}\,(p_y)/2 - \phi_p^+(x)$ tends to zero when x tends to a turning point x_0 and can therefore be treated as one-half of the angle around the origin in p-space accumulating during the motion of a classicle particle from the point x to the turning point x_0 and back. The peculiar behaviour of the phase difference can mathematicaly be expressed as the non-commutativity of limits:

$$\lim_{p_y\to\pm 0}\lim_{x\to x_0}[\phi_p^-(x)-\phi_p^+(x)] = 0,$$
$$\lim_{x\to x_0}\lim_{p_y\to\pm 0}[\phi_p^-(x)-\phi_p^+(x)] = \pm\pi. \tag{84}$$

The jump in the sign of the outgoing wave must be compensated for by a kink in the reflection coefficient, since the whole wavefunction should analytically depend on p_y. To get rid of the jump, one can redefine the outgoing wave and write [42]

$$\psi(x) = \frac{|E-u(x)|^{1/2}}{\left[(E-u(x))^2 - p_y^2\right]^{1/4}} \times (\mathrm{e}^{\mathrm{i}S^+(x)/h+\mathrm{i}\phi_p^+(x)/2} + r(p_y)\mathrm{e}^{-\mathrm{i}S^+(x)/h-\mathrm{i}\phi_p^+(x)/2}). \tag{85}$$

Although preserving the analyticity of $r(p_y)$, such a definition introduces an artificial jump of the phase as a function of x upon reflection at negative p_y. Therefore, we do not use it below.

The reflection coefficient, defined in accordance with (80) and (81), does not depend on the sign of p_y. It is completely defined by the orientation of the phase space, which is clockwise for an electron region and counterclockwise for a hole region (see figure 1). Finally, the reflection can be written as

$$r(p_y) = \mathrm{e}^{\mp\mathrm{i}\pi/2}, \tag{86}$$

where '−' corresponds to electron and '+' to hole regions.

It is important to note that the phase $-\pi/2$ and the modulus 1 of the reflection coefficient (86) were obtained under the assumption that there is no multiplicity change! It is not the case when $p_y \to 0$ and the trajectory in the phase space tends to a separatrix; see figure 2.

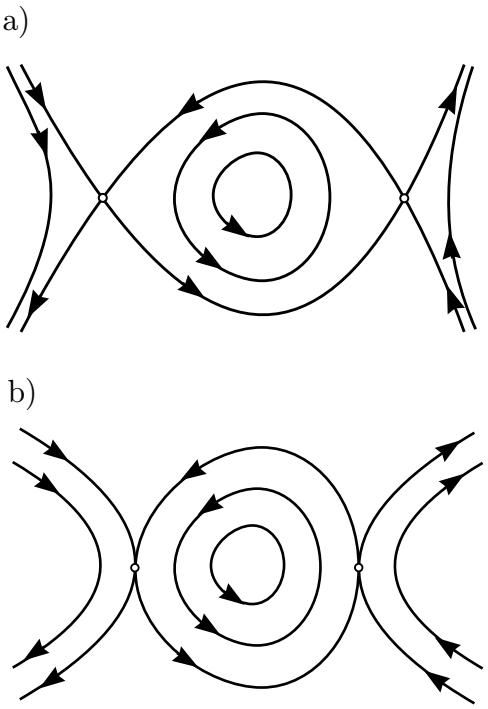

Figure 2. Classical phase space for n–p–n junction in (a) single and (b) bilayer graphene. Different trajectories correspond to different values of p_y. One finds that for normal incidence (separatrices) the smoothest classical trajectory corresponds to total transmission in single-layer graphene and to total reflection in bilayer graphene.

Let us now turn to bilayer graphene. The Hamiltonian describing the charge carrier dynamics reads

$$H = \begin{pmatrix} 0 & (\hat{p}_x - \mathrm{i}p_y)^2 \\ (\hat{p}_x + \mathrm{i}p_y)^2 & 0 \end{pmatrix} + u(x). \tag{87}$$

Eigenvalues and eigenvectors of $H(p_x, x)$ are

$$L_0^\pm = \pm p^2 + u(x), \qquad \chi_0^\pm = \frac{1}{\sqrt{2}}\begin{pmatrix} \mathrm{e}^{-2\mathrm{i}\phi_p} \\ \pm 1 \end{pmatrix}. \tag{88}$$

We obtain

$$\psi(x) = \frac{1}{\left|E-u(x)\mp p_y^2\right|^{1/4}}\mathrm{e}^{\pm\mathrm{i}S^+(x)/h+\mathrm{i}\phi_p^\pm(x)},$$
$$S(x) = \int_{x_0}^{x}\sqrt{\pm[E-u(x)]-p_y^2}\,\mathrm{d}x. \tag{89}$$

Obviously, the result (86) is valid for the bilayer as well, since the orientation of the phase space is the same.

Between two classically forbidden regions, effective Hamiltonians superimpose the following quantization conditions (see appendix C for details):

$$\frac{1}{h}\oint p_x\,\mathrm{d}x + \frac{\beta}{2}\Delta\phi_p = 2\pi\left(n+\frac{\nu}{4}\right), \tag{90}$$

where $\beta = 1, 2$ for single and bilayer, respectively, $\nu = 2$ is the Maslov index and $\Delta\phi_p$ is the total phase gain along the closed classical trajectory. The term $\beta\Delta\phi_p/2$ is the Berry phase in graphene [43]. It is clear that $\Delta\phi_p$ acquires a non-zero value only if the trajectory in p-space encloses the origin. Therefore in the absence of magnetic field $\Delta\phi_p = 0$. Quantization condition (90) allows one to determine resonance angles.

Although the considered diagonalization is very powerful to deal with complicated matrix Hamiltonians in a classically allowed region, it possesses a considerable disadvantage: it treats electrons and holes separately, neglecting tunneling effects. In the classically forbidden region when $|p| = 0$, i.e. $p_x = \mathrm{i}p_y$, effective Hamiltonians $L_0^{\pm}$ become degenerate. At this point, electron-to-hole transition may occur and the diagonalization fails. This transition is the origin of Klein tunneling.

8. Normal incidence

In the case of normal incidence $p_y = 0$ and at the point x_0, where $u(x_0) = E$, there is a multiplicity change, i.e. effective Hamiltonians $L_0^{\pm}$ become degenerate (see figure 2). To study wavefunctions in this case, one cannot apply a standard semiclassical treatment, described in section 7 since there may be a 'jump' between L^+ and L^-. Fortunately, for the normal incidence in graphene there is an exact pseudospin conservation, which allows one to study this case in detail.

For $p_y = 0$, equations (62) and (63) read

$$[\sigma_x\hat{p}_x^{\beta} + u(x) - E]\Psi = 0, \tag{91}$$

where $\beta = 1$, 2 for single and bilayer, respectively. Eigenvectors of $\sigma_x\hat{p}_x^{\beta}$ do not depend on $\hat{p}_x^{\beta}$; therefore (91) can be easily diagonalized, which leads to

$$[\pm\hat{p}_x^{\beta} + u(x) - E]\eta_{1,2} = 0, \tag{92}$$

where

$$\Psi = \begin{pmatrix}1\\1\end{pmatrix}\eta_1 + \begin{pmatrix}1\\-1\end{pmatrix}\eta_2. \tag{93}$$

In this case, the eigenvalue of σ_x ('pseudospin') persists. Pseudospin conservation leads to very different physical consequences for single-layer and bilayer graphene.

For single-layer graphene, pseudospin conservation means the conservation of the x-component of the velocity. Equation (92) is a first-order differential equation, which can be solved exactly. We obtain

$$\eta_{1,2} = C_{1,2}\exp\left(\pm\mathrm{i}\int_{x_0}^{x}[E - u(x')]\mathrm{d}x'\right), \tag{94}$$

where $C_{1,2}$ are some constants. The absence of the reflected wave in (94) means that for any potential shape, one has perfect transmission. Thus we conclude that at the point $p_x = 0$, there is a *total transition* between electron and hole states since Hamiltonians (68) depend on $|p|$ in contrast with (92)!

For bilayer graphene, pseudospin conservation is equivalent to the conservation of particle type, as is seen from the comparison of (88) and (92). Therefore, an incoming particle obeys the Schrödinger equation (92) everywhere. For a 'Klein-setup' this leads to exponentially decaying transmission as a function of potential width and height.

Total transmission for normally incident electrons in single-layer graphene and its exponential damped behavior in bilayer have natural explanations in terms of classical phase space (figure 2). In both cases the most probable process corresponds to the smoothest trajectory, constructed from separatrix pieces. For a single layer, such a trajectory goes through the barrier and gives total transmission, while for a bilayer, one has to choose the trajectory reflected from the barrier to avoid discontinuity in the second derivative of x with respect to p_x.

9. Exact reduction to effective Schrödinger equations

In section 7, it was mentioned that the standard adiabatic diagonalization fails to describe Klein tunneling, since it treats electrons and holes separately. However, the existence of exact diagonalization (section 8) for normal incidence raises the issue of a possible generalization for angular scattering. We shall show that for single-layer graphene there exists an *exact* transformation, reducing the original Dirac equation to a scalar Schrödinger-like equation with a *complex* potential. It is clear that such a procedure cannot be a unitary transformation of the original Hermitian Hamiltonian.

Let us return to the Dirac equation for a single layer and write it in the form

$$(\boldsymbol{\sigma p} + v(x))\Psi = 0, \tag{95}$$

where $\boldsymbol{p} = (\hat{p}_x, p_y)$, $v(x) = u(x) - E$. Let us act on the last equation from the left by the operator $\boldsymbol{\sigma p} - v(x)$. Then we obtain

$$\begin{aligned}(\boldsymbol{\sigma p} - v(x))(\boldsymbol{\sigma p} + v(x))\Psi &= (\hat{p}_x^2 + p_y^2 - v(x)^2 + \sigma_x[\hat{p}_x, v(x)])\Psi\\ &= (\hat{p}_x^2 + p_y^2 - v(x)^2 - \mathrm{i}h\sigma_x v'(x))\Psi\\ &= 0.\end{aligned} \tag{96}$$

Remarkably, (96) contains only the single matrix σ_x. Therefore, it can be easily diagonalized. We write

$$\Psi = \begin{pmatrix}1\\1\end{pmatrix}\eta_1 + \begin{pmatrix}1\\-1\end{pmatrix}\eta_2 \tag{97}$$

and obtain

$$\left(h^2\frac{\mathrm{d}^2}{\mathrm{d}x^2} + v(x)^2 - p_y^2 \pm \mathrm{i}hv'(x)\right)\eta_{1,2} = 0. \tag{98}$$

Functions $\eta_{1,2}$ are not independent and the connection formula can be obtained from (95). The function η_2 can be reconstructed from η_1 as

$$\eta_2 = \frac{1}{p_y}\left(h\frac{\mathrm{d}}{\mathrm{d}x} + \mathrm{i}v(x)\right)\eta_1. \tag{99}$$

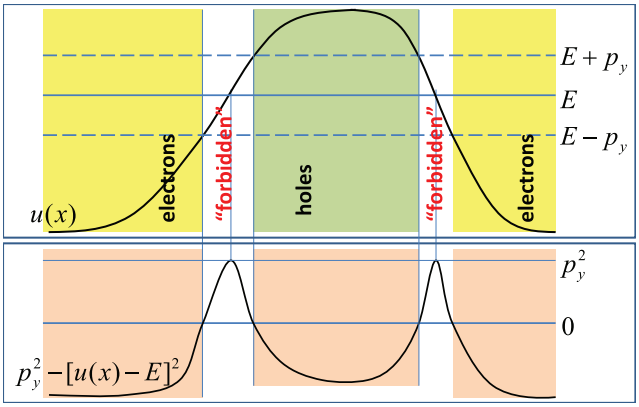

Figure 3. Comparison of the initial potential with the real part of the effective potential.

In figure 3, one sees the initial potential landscape and the real part of the effective potential in (98). Although this equation takes the form of a Schrödinger equation, there are two substantial distinctions as compared to a common Schrödinger particle: (i) the effective potential is complex and (ii) it depends on energy.

10. Single n–p junction

10.1. Exact solution in the case of a linear n–p junction

Let us first consider an exactly solvable model for a linear potential $v(x)=\alpha x$, $\alpha>0$ [44]. Introducing a new variable $x'=(\alpha/h)^{1/2}x$ and a new y-component of the momentum $p_y'=(h\alpha)^{-1/2}p_y$, we exclude h and α from (98). Then it takes the form (we omit primes)

$$\left(\frac{\mathrm{d}^2}{\mathrm{d}x^2}+x^2-p_y^2+\mathrm{i}\right)\eta_1=0. \tag{100}$$

Introducing a new variable z such that $x=\xi z$, we have

$$\left(\frac{\mathrm{d}^2}{\mathrm{d}z^2}+\xi^2(\mathrm{i}-p_y^2)+\xi^4z^2\right)\eta_1=0. \tag{101}$$

Choosing an appropriate value for ξ, we can reduce (101) to Weber's equation [45]

$$w''(z)+\left(\nu+\frac{1}{2}-\frac{z^2}{4}\right)w(z)=0. \tag{102}$$

Indeed, choosing $\xi=\mathrm{e}^{-\mathrm{i}\pi/4}/\sqrt{2}$ and solving Weber's equation [45, 46], we obtain

$$\eta_1=c_1D_\nu(\sqrt{2}\,\mathrm{e}^{\mathrm{i}\pi/4}x)+c_2D_{-\nu-1}(\sqrt{2}\,\mathrm{e}^{3\mathrm{i}\pi/4}x), \tag{103}$$

where $\nu=\mathrm{i}p_y^2/2$ and D_ν are the parabolic cylinder functions. For these functions, the following identities hold:

$$\begin{aligned}\frac{\partial D_\nu(z)}{\partial z}&=\nu D_{\nu-1}(z)-\frac{z}{2}D_\nu(z),\\ \frac{\partial D_\nu(z)}{\partial z}&=\frac{z}{2}D_\nu(z)-D_{\nu+1}(z).\end{aligned} \tag{104}$$

Applying the first equality from (104), we find that

$$\left(\frac{\partial}{\partial x}+\mathrm{i}x\right)D_\nu(\sqrt{2}\,\mathrm{e}^{\mathrm{i}\pi/4}x)=\sqrt{2}\nu\,\mathrm{e}^{\mathrm{i}\pi/4}D_{\nu-1}(\sqrt{2}\,\mathrm{e}^{\mathrm{i}\pi/4}x). \tag{105}$$

From the second equality in (104), we have

$$\left(\frac{\partial}{\partial x}+\mathrm{i}x\right)D_{-\nu-1}(\sqrt{2}\,\mathrm{e}^{3\mathrm{i}\pi/4}x)=\sqrt{2}\,\mathrm{e}^{-\mathrm{i}\pi/4}D_{-\nu}(\sqrt{2}\,\mathrm{e}^{3\mathrm{i}\pi/4}x). \tag{106}$$

Substituting (105) and (106) into (99), we obtain

$$\begin{aligned}\eta_2&=\frac{1}{p_y}\left(\frac{\mathrm{d}}{\mathrm{d}x}+\mathrm{i}x\right)\eta_1\\ &=\frac{c_1}{p_y}\sqrt{2}\nu\,\mathrm{e}^{\mathrm{i}\pi/4}D_{\nu-1}(\sqrt{2}\,\mathrm{e}^{\mathrm{i}\pi/4}x)\\ &\quad+\frac{c_2}{p_y}\sqrt{2}\,\mathrm{e}^{-\mathrm{i}\pi/4}D_{-\nu}(\sqrt{2}\,\mathrm{e}^{3\mathrm{i}\pi/4}x).\end{aligned} \tag{107}$$

From (103) and (107), we have, for $\Psi=(\psi_1,\psi_2)$,

$$\begin{aligned}&\psi_{1,2}(x)=\eta_1(x)\pm\eta_2(x)\\ &=c_1\left(D_\nu(\sqrt{2}\,\mathrm{e}^{\mathrm{i}\pi/4}x)\pm\frac{\sqrt{2}\nu\,\mathrm{e}^{\mathrm{i}\pi/4}}{p_y}D_{\nu-1}(\sqrt{2}\,\mathrm{e}^{\mathrm{i}\pi/4}x)\right)\\ &\quad+c_2\left(D_{-\nu-1}(\sqrt{2}\,\mathrm{e}^{3\mathrm{i}\pi/4}x)\pm\frac{\sqrt{2}\,\mathrm{e}^{-\mathrm{i}\pi/4}}{p_y}D_{-\nu}(\sqrt{2}\,\mathrm{e}^{3\mathrm{i}\pi/4}x)\right).\end{aligned} \tag{108}$$

Using the asymptotic expansions of the parabolic cylinder functions (see appendix D), we find that when $x\to\infty$ (hole region)

$$\begin{aligned}\psi_{1,2}&\to c_1z_1^\nu\,\mathrm{e}^{-\mathrm{i}x^2/2}\\ &\quad+c_2\left[-\frac{\sqrt{2\pi}}{\Gamma(\nu+1)}z_2^\nu\,\mathrm{e}^{-\mathrm{i}x^2/2+\mathrm{i}\pi(\nu+1)}\pm\frac{\sqrt{2}\mathrm{e}^{-\mathrm{i}\pi/4}}{p_y}z_2^{-\nu}\mathrm{e}^{\mathrm{i}x^2/2}\right],\end{aligned} \tag{109}$$

and when $x\to-\infty$ (electron region)

$$\begin{aligned}\psi_{1,2}&\to c_1\left[(\bar{z}_2)^\nu\,\mathrm{e}^{-\mathrm{i}x^2/2}\pm\frac{\sqrt{2\pi}}{\Gamma(1-\nu)}\frac{\sqrt{2}\nu\,\mathrm{e}^{\mathrm{i}\pi/4}}{p_y}(\bar{z}_2)^{-\nu}\,\mathrm{e}^{\mathrm{i}x^2/2-\mathrm{i}\pi\nu}\right]\\ &\quad\pm c_2\frac{\sqrt{2}\,\mathrm{e}^{-\mathrm{i}\pi/4}}{p_y}(\bar{z}_1)^{-\nu}\,\mathrm{e}^{\mathrm{i}x^2/2},\end{aligned} \tag{110}$$

where $z_1=\sqrt{2}\,\mathrm{e}^{\mathrm{i}\pi/4}|x|$, $z_2=\sqrt{2}\,\mathrm{e}^{3\mathrm{i}\pi/4}|x|$ and a bar means complex conjugation.

Now we turn to a discussion of the scattering problem. While tunneling through the barrier the Dirac particle turns from an electron to a hole or vice versa. The x-component of the group velocity of the hole $v_x=\partial L_0^-/\partial p_x=-p_x/p$ has opposite sign with respect to its momentum p_x. Let us consider an electron coming from $-\infty$ with a positive velocity v_x. It corresponds to the action $S^+(x)\simeq-x^2/2$, since $p_x=\partial S^+(x)/\partial x\simeq-x>0$ and $v_x=p_x/p>0$. Thus, the reflected

electron corresponds to $S^-(x) \simeq x^2/2$. The transmitted hole with a positive velocity has a negative momentum p_x. Hence it corresponds to the action $S^-(x) \simeq -x^2/2$. From the absence of the incoming wave in the hole region, we find that $c_2 = 0$.

Let us consider (81) at infinity. Then we have for the action,

$$S^+(x) = \int_{\mathrm{sgn}\,(x)|p_y|}^{x} \sqrt{y^2 - p_y^2}\,\mathrm{d}y = \frac{1}{2}\mathrm{sgn}\,(x)\left\{|x|\sqrt{x^2-p_y^2} - p_y^2 \ln\left[\left|\frac{x}{p_y}\right| + \sqrt{\left(\frac{x}{p_y}\right)^2 - 1}\right]\right\}, \tag{111}$$

where we have assumed that $|x| > |p_y|$. For large x we obtain

$$S^+(x) \simeq \frac{1}{2}\mathrm{sgn}\,(x)\left\{x^2 - \frac{p_y^2}{2} - p_y^2 \ln\left(\frac{2|x|}{|p_y|}\right)\right\}. \tag{112}$$

Thus for large negative x, (81) reads

$$\Psi(x) = \mathrm{e}^{-\mathrm{i}x^2/2 + \mathrm{i}p_y^2/4 + (\mathrm{i}/2)p_y^2 \ln(2|x|/|p_y|)}\begin{pmatrix}1\\1\end{pmatrix} + r(p_y)\mathrm{e}^{\mathrm{i}x^2/2 - \mathrm{i}p_y^2/4 - (\mathrm{i}/2)p_y^2 \ln(2|x|/|p_y|)}\begin{pmatrix}\mathrm{e}^{-\mathrm{i}\pi\,\mathrm{sgn}\,(p_y)/2}\\ \mathrm{e}^{\mathrm{i}\pi\,\mathrm{sgn}\,(p_y)/2}\end{pmatrix}. \tag{113}$$

This gives for the reflection

$$r(p_y) = \frac{\sqrt{\pi}|p_y|}{\Gamma(1-\nu)}\mathrm{e}^{-\pi p_y^2/4}\,\mathrm{e}^{\mathrm{i}\theta(p_y) - \mathrm{i}\pi/2}, \tag{114}$$

where $\theta(p_y) = p_y^2/2 - (p_y^2/2)\ln(p_y^2/2) - \pi/4$. Using equalities

$$|\Gamma(1-\nu)|^2 = \Gamma(1-\nu)\Gamma(1+\nu) = \nu\Gamma(\nu)\Gamma(1-\nu) = \frac{\pi\nu}{\sin(\pi\nu)} = \frac{\pi p_y^2}{\mathrm{e}^{\pi p_y^2/2} - \mathrm{e}^{-\pi p_y^2/2}}, \tag{115}$$

we can write the reflection coefficient as

$$r(p_y) = \sqrt{1 - \mathrm{e}^{-\pi p_y^2}}\,\mathrm{e}^{\mathrm{i}\theta(p_y) - \mathrm{i}\gamma(p_y) - \mathrm{i}\pi/2}, \tag{116}$$

where $\gamma(p_y) = \arg\Gamma(1 - \mathrm{i}p_y^2/2)$. From the asymptotic expansion of the Γ-function at large arguments [45], one concludes that $\gamma(p_y)$ tends to $\theta(p_y)$ when p_y tends to infinity. At small p_y the reflection coefficient is proportional to $|p_y|$. This nonanalytic behavior is compensated for by the jump in the phase of the reflected wave as we discussed in section 7.

Comparing the coefficient in front of incoming and transmitted waves, we find for the transmission amplitude

$$t = \mathrm{e}^{\mathrm{i}\pi\,\mathrm{sgn}\,(p_y)/2}\,\mathrm{e}^{\mathrm{i}\pi\nu} = \mathrm{e}^{\mathrm{i}\pi\,\mathrm{sgn}\,(p_y)/2}\,\mathrm{e}^{-\pi p_y^2/2}. \tag{117}$$

For the transmission probability, we thus have

$$|t|^2 = \mathrm{e}^{-\pi p_y^2} = \mathrm{e}^{-\pi p^2 \sin^2\phi_p}. \tag{118}$$

This result was first obtained by Cheianov and Fal'ko [44]. Considering the scattering from the right to the left, we find that the transmission amplitude in this case is

$$t = -\mathrm{e}^{-\mathrm{i}\pi\,\mathrm{sgn}\,(p_y)/2}\,\mathrm{e}^{-\pi p_y^2/2}. \tag{119}$$

The transfer matrix connecting incoming and outgoing waves from the right to the left of the barrier for positive α is

$$T_+ = \mathrm{e}^{-\mathrm{i}\pi\,\mathrm{sgn}\,(p_y)/2} \times \begin{pmatrix} \mathrm{e}^{\pi p_y^2/2} & (\mathrm{e}^{\pi p_y^2} - 1)^{1/2}\,\mathrm{e}^{\mathrm{i}(\gamma - \theta - \pi/2)} \\ (\mathrm{e}^{\pi p_y^2} - 1)^{1/2}\,\mathrm{e}^{\mathrm{i}(\theta - \gamma - \pi/2)} & -\mathrm{e}^{\pi p_y^2/2}\end{pmatrix}. \tag{120}$$

For negative α the transfer matrix reads

$$T_- = \mathrm{e}^{-\mathrm{i}\pi\,\mathrm{sgn}\,(p_y)/2} \times \begin{pmatrix} -\mathrm{e}^{\pi p_y^2/2} & (\mathrm{e}^{\pi p_y^2} - 1)^{1/2}\,\mathrm{e}^{\mathrm{i}(\theta - \gamma - \pi/2)} \\ (\mathrm{e}^{\pi p_y^2} - 1)^{1/2}\,\mathrm{e}^{\mathrm{i}(\gamma - \theta - \pi/2)} & \mathrm{e}^{\pi p_y^2/2}\end{pmatrix}. \tag{121}$$

10.2. Transmission probability in the semiclasical approximation

Let us consider an outgoing hole on the right of a generic potential monotonically growing from left to right. In the semiclassical approximation, it is described by the wavefunction

$$\Psi(x) = \frac{\mathrm{e}^{-\mathrm{i}\pi\,\mathrm{sgn}\,(p_y)/2}|E - u(x)|^{1/2}}{\left[(E-u(x))^2 - p_y^2\right]^{1/4}}\mathrm{e}^{-\mathrm{i}S^+(x)/h}\begin{pmatrix}\mathrm{e}^{\mathrm{i}\phi_p^+(x)/2}\\ \mathrm{e}^{-\mathrm{i}\phi_p^+(x)/2}\end{pmatrix}. \tag{122}$$

Using equalities

$$\cos\left(\frac{\phi_p^+}{2}\right) = \sqrt{\frac{1+\cos\phi_p^+}{2}}, \quad \sin\left(\frac{\phi_p^+}{2}\right) = \mathrm{sgn}(p_y)\sqrt{\frac{1-\cos\phi_p^+}{2}},$$
$$\cos\phi_p^+ = \frac{|p_x|}{|p|} = \frac{[(E-u(x))^2 - p_y^2]^{1/2}}{|E-u(x)|}, \tag{123}$$

we write it as

$$\Psi(x) = \frac{\mathrm{e}^{-\mathrm{i}\pi\,\mathrm{sgn}\,(p_y)/2}}{\left[v^2 - p_y^2\right]^{1/4}\left[v + \sqrt{v^2 - p_y^2}\right]^{1/2}} \times \mathrm{e}^{-\mathrm{i}S^+/h}\begin{pmatrix} v + \sqrt{v^2 - p_y^2} + \mathrm{i}p_y \\ v + \sqrt{v^2 - p_y^2} - \mathrm{i}p_y\end{pmatrix} \tag{124}$$

with $v(x) = u(x) - E$. According to (124), the components of $\Psi(x)$ can be represented *exactly* as a sum or a difference of functions η_1 and η_2 obeying Schrödinger-like equations (98) with a complex potential. Despite the complexity of the potential, according to [47], to connect a transmitted wave on the right of the barrier with an incoming wave on the left of the barrier one can still use an analytic continuation in the classically forbidden region similar to [48]. In contrast with a usual Schrödinger equation the transmitted hole has a negative momentum, so $\Psi(x)$ in (122) is proportional to $\mathrm{e}^{-\mathrm{i}S^+/h}$, but not to $\mathrm{e}^{\mathrm{i}S^+/h}$. Therefore the passage should be done in the

lower complex half-plane. Since both functions η_1 and η_2 allow analytic continuations in the lower half-plane, $\Psi(x)$ can also be continued in the lower half-plane.

Performing the passage and connecting the outgoing wave with an incoming wave, we obtain for the transmission coefficient

$$t = \mathrm{e}^{\mathrm{i}\pi\,\mathrm{sgn}\,(p_y)/2}\,\mathrm{e}^{-K/h}, \quad K = \left|\int_{x_1}^{x_2}\sqrt{p_y^2 - v^2(x)}\mathrm{d}x\right|, \quad (125)$$

where x_1 and x_2 are two turning points, i.e. solutions for the equation $p_y^2 - v^2(x) = 0$. The standard complex Wentzel–Kramers–Brillouin (WKB) technique [47, 49, 50] does not allow one to compute the reflection coefficient with exponential accuracy. The modulus of the reflection coefficient can be computed from the unitarity of the scattering matrix: $|r|^2 + |t|^2 = 1$. This gives

$$|r| = \sqrt{1 - \mathrm{e}^{-2K/h}}. \quad (126)$$

The semiclassical phase of the reflection coefficient can be reconstructed from (82) and (83). Thus in the semiclassical approximation we obtain

$$r = \sqrt{1 - \mathrm{e}^{-2K/h}}\,\mathrm{e}^{\mp\mathrm{i}\pi/2}, \quad (127)$$

where '−' corresponds to the electron and '+' to the hole region. For small p_y any potential can be linearized in the classically forbidden region. Comparing (117) and (125), we see that in the limit $p_y \to 0$ the semiclassical transmission becomes exact. Therefore (125) can be used as a uniform approximation for the transmission coefficient at any p_y. Then the uniform approximation for the reflection coefficient reads

$$r = \sqrt{1 - \mathrm{e}^{-2K/h}}\,\mathrm{e}^{\mp\mathrm{i}\pi/2+\mathrm{i}\Theta}, \quad (128)$$

where Θ tends to zero when p_y tends to infinity. For the phase Θ, we used the expression [51, 52]

$$\Theta = \frac{K}{\pi h} - \frac{K}{\pi h}\ln\left(\frac{K}{\pi h}\right) - \frac{\pi}{4} - \arg\Gamma\left(1 - \frac{\mathrm{i}K}{\pi h}\right), \quad (129)$$

which was obtained by the replacement $\pi p_y^2/2$ by K/h in $\theta(p_y) - \gamma(p_y)$.

11. Klein tunneling in n–p–n junctions: the Fabry–Pérot interferometer

Let us consider some generic potential barrier $u(x)$. In graphene it implies an n–p–n junction (see figure 3). In terms of (98), an n–p–n junction becomes a complex double-hump potential. The transfer matrix in this case is

$$T = T_+\begin{pmatrix}\mathrm{e}^{\mathrm{i}S/h} & 0\\ 0 & \mathrm{e}^{-\mathrm{i}S/h}\end{pmatrix}T_-, \quad S = \int_{x_2}^{x_3}\sqrt{v^2(x) - p_y^2}\,\mathrm{d}x, \quad (130)$$

where we assume that $x_2 < x_3$. There is no extra phase coming from $\phi_p^{\pm}$ since each of these functions takes the same values

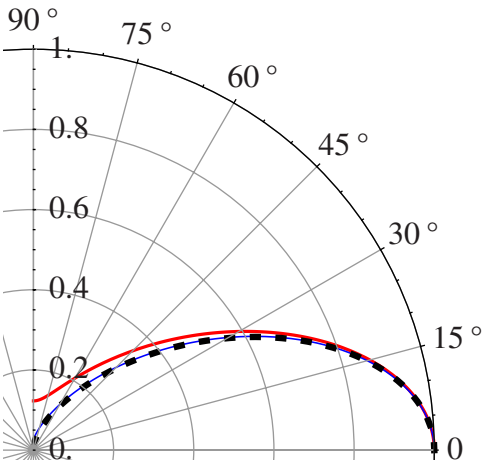

Figure 4. The angular dependence of the transmission coefficient for a particle of energy 80 meV incident on an n–p junction of height 200 meV. The potential is given by equation (135), with $l_1 = 70$ nm. The blue line shows the numerical result with 49 steps, the dashed line shows the semiclassical result (125) and the red line shows the result for a linear potential (117), where the parameter α was taken as the derivative at the central point of the junction.

at both turning points x_2, x_3 lying in the hole region. The transmission coefficient reads

$$t = \frac{1}{T_{11}} = -\frac{\mathrm{e}^{-\mathrm{i}S/h}\,\mathrm{e}^{-K_1/h - K_2/h}}{1 + \mathrm{e}^{-2\mathrm{i}S/h - \mathrm{i}\Theta_1 - \mathrm{i}\Theta_2}\sqrt{1 - \mathrm{e}^{-2K_1/h}}\sqrt{1 - \mathrm{e}^{-2K_2/h}}}. \quad (131)$$

The obtained transmission amplitude can easily be treated in terms of the sum of the probability amplitudes of multiscattering processes leading to transmission [42]. One sees that for normal incidence $K_1 = K_2 = 0$ and the modulus of the transmission coefficient becomes 1. Transmission resonances can be found from the condition

$$\frac{S}{h} + \frac{\Theta_1 + \Theta_2}{2} = \pi\left(n + \frac{1}{2}\right), \quad (132)$$

which coincides with the quantization condition (90) for large p_y. For a symmetric n–p–n junction, the resonant transmission is always one, since $K_1 = K_2$. For an asymmetric junction, resonant values of transmission decay as

$$|t| \sim \frac{1}{\cosh(K_1/h - K_2/h)} \quad (133)$$

when $K_1/h \gg 1$ and $K_2/h \gg 1$. From (133) one sees that resonant values of transmission exponentially decay as a function of $|K_1 - K_2|$. Such a fast decay can be crucial if one wants to weaken the influence of side resonances.

12. Numerical results

In figures 4–6, we compare our semiclassical predictions with numerical results, obtained from a multistep approximation of the initial potential. A check on the accuracy of the calculation for constant p_y is provided by the current

$$j_x = \Psi^{\dagger}\sigma_x\Psi, \quad \mathrm{d}\,j_x/\mathrm{d}x = 0. \quad (134)$$

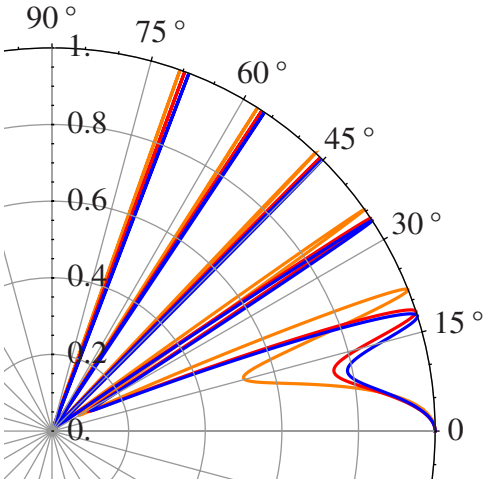

Figure 5. The angular dependence of the transmission coefficient for a particle of energy 80 meV incident on an n–p–n junction of height 200 meV. The barrier width $l_2 = 250$ nm and n–p and p–n regions have characteristic lengths $l_1 = l_3 = 100$ nm. The blue line shows the numerical result for 99 steps, the red line shows the uniform approximation (131) and the orange line shows the semiclassical answer ($\Theta_1 = \Theta_2 = 0$).

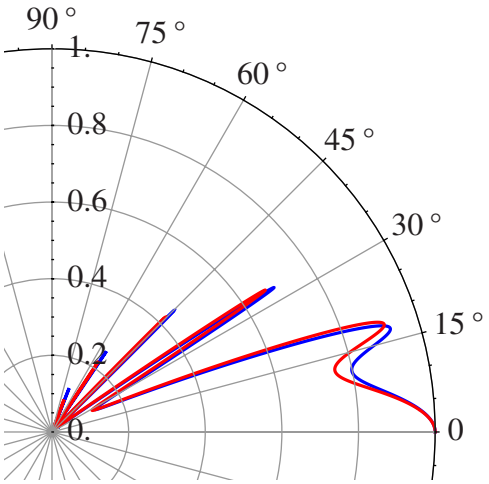

Figure 6. The angular dependence of the transmission coefficient for a particle of energy 80 meV incident on an n–p–n junction of height 200 meV. The barrier width $l_2 = 250$ nm and the n–p and p–n regions have characteristic lengths $l_1 = 150$ nm and $l_3 = 50$ nm, respectively. The blue line shows the numerical results for 99 steps, while the red line shows the uniform approximation (131).

To simulate an n–p junction we used the potential

$$V(x/l_1) = 0.5\, U_{\max}\,[1 + \tanh(10x/l_1 - 5)] \tag{135}$$

with a characteristic length scale l_1. An n–p–n junction was simulated as an n–p junction with a characteristic length l_1, a p–n junction with a characteristic length l_3 and a constant potential in between of length l_2.

In figure 4, we show the comparison of our numerical result for an n–p junction with the semiclassical transmission (125) and the transmission for a linear potential (117). While the semiclassical prediction works uniformly over the entire range of angles, the prediction obtained from a linear potential works only for small angles.

In figure 5, we show the comparison of our numerical results with the prediction (131) for a symmetric n–p–n junction. We also show the semiclassical result, which is obtained by setting $\Theta_1 = \Theta_2 = 0$. The agreement between the latter answer and numerics gets better as the angle increases, i.e. deep in the semiclassical regime. The result (125) uniformly approximates the numerical data over the entire range of angles.

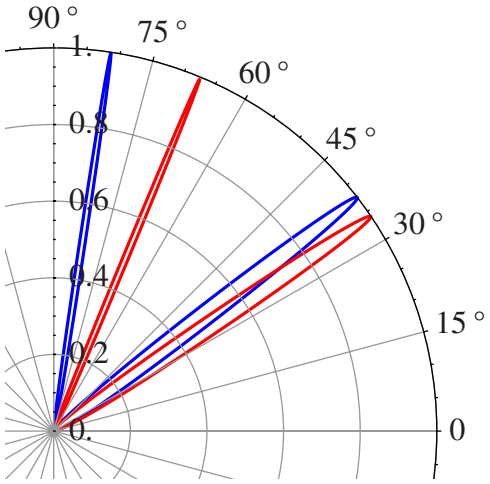

Figure 7. The angular dependence of the transmission coefficent for a particle of energy 17 meV incident on symmetric and asymmetric n–p–n junctions in bilayer graphene. Each junction is of height 50 meV and width $l_2 = 100$ nm. The blue line shows the numerical result for a symmetric junction with $l_1 = l_3 = 10$ nm, while the red line shows that for an asymmetric junction with $l_1 = 20$ nm and $l_3 = 40$ nm. All calculations were performed with 99 steps per junction.

In figure 6, the result for an asymmetric n–p–n junction is shown. The height of resonances is seen to decay. The *suppression of side resonances for asymmetric junctions* in single-layer graphene can have essential consequences for attemps to confine Dirac particles!

Numerical computations for bilayer graphene using the above procedure are less accurate, due to the presence of real exponentials everywhere. Therefore we were unable to check the quantization condition (90) numerically with a high precision. To check the accuracy of the computation we used the current

$$j_x = \psi_1 \left(\frac{\mathrm{d}}{\mathrm{d}x} + k_y\right)\psi_2^* - \psi_2^* \left(\frac{\mathrm{d}}{\mathrm{d}x} - k_y\right)\psi_1$$
$$+\psi_2 \left(\frac{\mathrm{d}}{\mathrm{d}x} - k_y\right)\psi_1^* - \psi_1^* \left(\frac{\mathrm{d}}{\mathrm{d}x} + k_y\right)\psi_2, \quad \mathrm{d}\, j_x/\mathrm{d}x = 0. \tag{136}$$

In figure 7, we show our numerical results for a symmetric and an asymmetric n–p–n junction with the same shape of the potential as before. In contrast with the case of a single layer, resonances *do not seem to decay*.

13. Conclusion

Let us summarize our main results. A detailed analysis of the reflection and transmission problem for the Dirac electrons shows essential differences from the conventional Schrödinger case, due to the role of the Berry phase. The

reflection coefficient turns out to be a nonanalytic function of the transverse momentum p_y vanishing as $|p_y|$ at $p_y \to 0$.

We have presented a complete treatment of the chiral tunneling for both single-layer and bilayer graphene in terms of a classical phase space. This gives a natural explanation of the complete transmission of a normally incident wave for a single layer and its exponentially damped transmission in a bilayer. We have also demonstrated that in the case of a non-symmetric n–p–n junction in single-layer graphene, there is total transmission only for normal incidence, and other maxima are suppressed. Our numerical studies show that in the case of a bilayer there are always magic angles with total transmission.

Acknowledgments

We are grateful to Sergey Dobrokhotov, Andrey Shafarevich, Anna Esina and Andrey Shytov for helpful discussions. We acknowledge financial support from the Stichting voor Fundamenteel Onderzoek der Materie (FOM), which is financially supported by the Nederlandse Organisatie voor Wetenschappelijk Onderzoek (NWO).

Appendix A. Effective Hamiltonians in the adiabatic approximation

In this part of the appendix, we show how to reduce in the adiabatic approximation an initial matrix Hamiltonian to a set of effective scalar Hamiltonians. Our consideration follows [38, 39].

Let us consider an eigenvalue problem for a Hermitian matrix Hamiltonian $\hat{H}$,

$$H(-\mathrm{i}h\,\mathrm{d}/\mathrm{d}x, x)\Psi(x) = E\Psi(x), \tag{A.1}$$

where we assume that $\hat{p}_x = -\mathrm{i}h\,\mathrm{d}/\mathrm{d}x$ acts first and x acts next. In what follows we always assume this operator ordering. Let us introduce a vector operator $\hat{\chi}$ and a scalar wavefunction ψ by the requirement

$$\Psi(x) = \chi(-\mathrm{i}h\,\mathrm{d}/\mathrm{d}x, x, h)\psi(x). \tag{A.2}$$

We want ψ to satisfy an eigenvalue problem

$$L(-\mathrm{i}h\,\mathrm{d}/\mathrm{d}x, x, h)\psi(x) = E\psi(x), \tag{A.3}$$

with an effective Hermitian Hamiltonian $\hat{L}$. Substituting (A.3) into (A.1) we obtain

$$(\hat{H}\hat{\chi} - \hat{\chi}\hat{L})\psi(x) = 0. \tag{A.4}$$

The last equality will be fulfilled for any $\psi(x)$ if the following operator equality holds:

$$H(-\mathrm{i}h\,\mathrm{d}/\mathrm{d}x, x)\chi(-\mathrm{i}h\,\mathrm{d}/\mathrm{d}x, x, h) = \chi(-\mathrm{i}h\,\mathrm{d}/\mathrm{d}x, x, h) \times L(-\mathrm{i}h\,\mathrm{d}/\mathrm{d}x, x, h). \tag{A.5}$$

We will solve it by passing to symbols of operators (see [40, 41]):

$$\mathrm{smb}[A(-\mathrm{i}h\,\mathrm{d}/\mathrm{d}x, x)B(-\mathrm{i}h\,\mathrm{d}/\mathrm{d}x, x)] = A(p_x - \mathrm{i}h\,\mathrm{d}/\mathrm{d}x, x) \times B(p_x, x). \tag{A.6}$$

Applying this formula to the above case, we obtain

$$H(p_x - \mathrm{i}h\,\mathrm{d}/\mathrm{d}x, x)\chi(p_x, x, h) = \chi(p_x - \mathrm{i}h\,\mathrm{d}/\mathrm{d}x, x, h) \times L(p_x, x, h). \tag{A.7}$$

Let us expand this expression with respect to the parameter $h \ll 1$. In zeroth order we obtain

$$H(p_x, x)\chi_0(p_x, x) = L_0(p_x, x)\chi_0(p_x, x), \tag{A.8}$$

where $L_0(p_x, x) = L(p_x, x, 0)$, $\chi_0(p_x, x) = \chi(p_x, x, 0)$. The first-order term in the expansion gives

$$-\mathrm{i}\frac{\partial H}{\partial p_x}\frac{\partial \chi_0}{\partial x} + H\chi_1 = -\mathrm{i}\frac{\partial \chi_0}{\partial p_x}\frac{\partial L_0}{\partial x} + L_0\chi_1 + \chi_0 L_1, \tag{A.9}$$

where L_1 and χ_1 are the first-order terms in L and χ with respect to h. The above expression can be rewritten as

$$(H - L_0)\chi_1 = \mathrm{i}\frac{\partial H}{\partial p_x}\frac{\partial \chi_0}{\partial x} - \mathrm{i}\frac{\partial \chi_0}{\partial p_x}\frac{\partial L_0}{\partial x} + \chi_0 L_1. \tag{A.10}$$

Let us multiply the last equation by $\chi_0^\dagger$ from the left. Since both H and L_0 are Hermitian matrices, we obtain

$$L_1 = -\mathrm{i}\chi_0^\dagger\frac{\partial H}{\partial p_x}\frac{\partial \chi_0}{\partial x} + \mathrm{i}\chi_0^\dagger\frac{\partial \chi_0}{\partial p_x}\frac{\partial L_0}{\partial x}, \tag{A.11}$$

where we have used the equality $\chi_0^\dagger\chi_0 = 1$.

Appendix B. Semiclassical approximation

B.1. The x-representation

To solve equation (A.3) we will use the semiclassical ansatz

$$\psi(x) = \mathrm{e}^{\mathrm{i}S(x)/h}A(x, h). \tag{B.1}$$

Then (A.3) can then be rewritten as

$$L(\mathrm{d}S/\mathrm{d}x - \mathrm{i}h\,\mathrm{d}/\mathrm{d}x, x, h)A(x, h) = EA(x, h). \tag{B.2}$$

This equation can be expanded order by order in x, which to zeroth order gives the Hamilton–Jacobi equation

$$L_0(\mathrm{d}S/\mathrm{d}x, x) = E. \tag{B.3}$$

From this equation, we can determine the action $S(x)$, as is well known from classical mechanics [53]. To first order in h we obtain the equation

$$-\mathrm{i}\frac{\partial L_0}{\partial p_x}\frac{\partial A_0}{\partial x} + L_1 A_0 - \frac{\mathrm{i}}{2}\frac{\partial^2 L_0}{\partial p_x^2}\frac{\mathrm{d}^2 S}{\mathrm{d}x^2}A_0 = 0, \tag{B.4}$$

where all terms should be evaluated at $p_x = \mathrm{d}S/\mathrm{d}x$. After multiplying by the amplitude A_0, equation (B.4) can be rewritten as

$$-\frac{\mathrm{i}}{2}\frac{d}{dx}\left(\frac{\partial L_0}{\partial p_x}A_0^2\right) + \left(L_1 + \frac{\mathrm{i}}{2}\frac{\partial^2 L_0}{\partial p_x \partial x}\right)A_0^2 = 0, \tag{B.5}$$

where the total derivative acts on both x and $p_x = \mathrm{d}S/\mathrm{d}x$. This equation can be solved exactly to determine the amplitude

$$A_0 = \left|\frac{\partial L_0}{\partial p_x}\right|^{-1/2} \exp\left[-\mathrm{i}\int \mathrm{d}x \left(\frac{\partial L_0}{\partial p_x}\right)^{-1}\left(L_1 + \frac{\mathrm{i}}{2}\frac{\partial^2 L_0}{\partial p_x \partial x}\right)\right] \tag{B.6}$$

$$\equiv \left|\frac{\partial L_0}{\partial p_x}\right|^{-1/2} \exp\left[\int \mathrm{d}x \left(\frac{\partial L_0}{\partial p_x}\right)^{-1} M\right], \tag{B.7}$$

where we have defined M. Using equation (A.11) it can be written as

$$M = -\chi_0^\dagger \frac{\partial H}{\partial p_x}\frac{\partial \chi_0}{\partial x} + \chi_0^\dagger \frac{\partial \chi_0}{\partial p_x}\frac{\partial L_0}{\partial x} + \frac{1}{2}\frac{\partial^2 L_0}{\partial p_x \partial x}. \tag{B.8}$$

B.2. The p-representation

We can also solve equation (A.3) by passing to p-representation [40, 41]:

$$L(\overset{1}{p_x}, \mathrm{i}h\overset{2}{\mathrm{d}}/\mathrm{d}p_x, h)\widetilde{\psi}(p_x) = E\widetilde{\psi}(p_x). \tag{B.9}$$

In this equation p_x acts first, while $\mathrm{i}h\,\mathrm{d}/\mathrm{d}p_x$ acts next, contrary to the case we considered before. To solve this equation, we use the semiclassical ansatz

$$\widetilde{\psi}(p_x) = \mathrm{e}^{-\mathrm{i}\widetilde{S}(p_x)/h}\widetilde{A}(p_x, h). \tag{B.10}$$

Similarly to equation (B.2) equation (B.9) can be rewritten as

$$L(p_x, \mathrm{d}\widetilde{S}/\mathrm{d}p_x + \mathrm{i}h\,\mathrm{d}/\mathrm{d}p_x, h)\widetilde{A}(p_x, h) = E\widetilde{A}(p_x, h). \tag{B.11}$$

When this equation is expanded order to order in h, one obtains to zeroth order the Hamilton–Jacobi equation

$$L_0(p_x, \mathrm{d}\widetilde{S}/\mathrm{d}p_x) = E, \tag{B.12}$$

from which the action $\widetilde{S}(p_x)$ can be determined. The first-order term becomes

$$\mathrm{i}\frac{\partial L_0}{\partial x}\frac{\partial \widetilde{A}_0}{\partial p_x} + L_1\widetilde{A}_0 + \frac{\mathrm{i}}{2}\frac{\partial^2 L_0}{\partial x^2}\frac{d^2\widetilde{S}}{\mathrm{d}p_x^2}\widetilde{A}_0 + \mathrm{i}\frac{\partial^2 L_0}{\partial x \partial p_x}\widetilde{A}_0 = 0, \tag{B.13}$$

where all terms have to be evaluated at $x = \mathrm{d}\widetilde{S}/\mathrm{d}p_x$. After multiplication by $\widetilde{A}_0$ one finds that

$$\frac{\mathrm{i}}{2}\frac{\mathrm{d}}{\mathrm{d}p_x}\left(\frac{\partial L_0}{\partial x}\widetilde{A}_0^2\right) + \left(L_1 + \frac{\mathrm{i}}{2}\frac{\partial^2 L_0}{\partial p_x \partial x}\right)\widetilde{A}_0^2 = 0, \tag{B.14}$$

which can be solved exactly to give

$$\widetilde{A}_0 = \left|\frac{\partial L_0}{\partial x}\right|^{-1/2} \exp\left[\mathrm{i}\int \mathrm{d}p_x \left(\frac{\partial L_0}{\partial x}\right)^{-1}\left(L_1 + \frac{\mathrm{i}}{2}\frac{\partial^2 L_0}{\partial p_x \partial x}\right)\right] \tag{B.15}$$

$$\equiv \left|\frac{\partial L_0}{\partial x}\right|^{-1/2} \exp\left[-\int \mathrm{d}p_x \left(\frac{\partial L_0}{\partial x}\right)^{-1} M\right]. \tag{B.16}$$

Using equation (A.11) the quantity M can then be written as

$$M = -\chi_0^\dagger \frac{\partial H}{\partial p_x}\frac{\partial \chi_0}{\partial x} + \chi_0^\dagger \frac{\partial \chi_0}{\partial p_x}\frac{\partial L_0}{\partial x} + \frac{1}{2}\frac{\partial^2 L_0}{\partial p_x \partial x}. \tag{B.17}$$

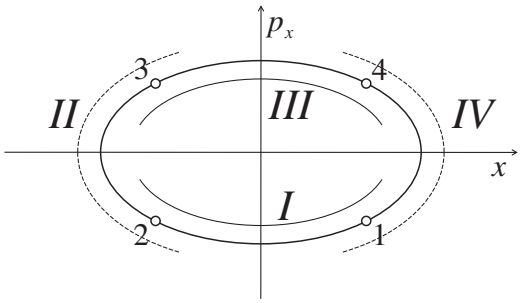

Figure C.1. The phase space of a classical particle is covered by maps I– IV. Regular maps I and III can be uniquely projected onto the x-axis, while singular maps II and IV can be uniquely projected onto the p_x-axis. The maps are chosen to overlap.

B.3. Matching

Since solutions (B.1) and (B.10) come from the same equation, they should be related. To find out what this relation is, we look at the Fourier representation of (B.1), which is defined by

$$\widetilde{\phi}(p_x) = \frac{1}{\sqrt{2\pi h}}\int_{-\infty}^{\infty} \mathrm{e}^{\mathrm{i}(S(x)-p_x x)/h}A_0(x)\,\mathrm{d}x. \tag{B.18}$$

Since the parameter h is assumed to be small, we can calculate this integral using the stationary phase method. The result is

$$\widetilde{\phi}(p_x) = \frac{A_0(x_s)}{\sqrt{|S''(x_s)|}}\mathrm{e}^{\mathrm{i}(S(x_s)-p_x x_s)/h + \mathrm{i}\,\mathrm{sgn}(S''(x_s))\,\pi/4}, \tag{B.19}$$

where the point $x_s = x_s(p_x)$ at which the phase is stationary is to be found from the equality

$$S'(x_s) = p_x. \tag{B.20}$$

From the comparison of (B.10) and (B.19), we find that [40, 41]

$$\widetilde{\phi}(p_x) = \mathrm{e}^{\mathrm{i}\,\mathrm{sgn}(S''(x_s))\,\pi/4}\widetilde{\psi}(p_x). \tag{B.21}$$

Appendix C. The Bohr–Sommerfeld quantization rule

Let us now consider the phase space that is shown in figure C.1.

Part I of the phase trajectory can be projected onto the x-axis. Therefore, we can use a standard WKB ansatz in this region. In contrast, in region II we can use a standard WKB ansatz in the p-representation. Since regions I and II overlap, functions are related according to (B.21). Since $S''(x_2) < 0$, we have $\psi_{\mathrm{I}}(x) \to \widetilde{\psi}_{\mathrm{II}}(p_x)\mathrm{e}^{-\mathrm{i}\pi/4}$.

It is easily seen that the above reasoning can also be applied to regions II and III. Since $S''(x_3) > 0$, we obtain $\psi_{\mathrm{III}}(x) \to \widetilde{\psi}_{\mathrm{II}}(p_x)\,\mathrm{e}^{\mathrm{i}\pi/4}$, or

$$\psi_{\mathrm{I}}(x) \to \psi_{\mathrm{III}}(x)\mathrm{e}^{-\mathrm{i}\pi/2}. \tag{C.1}$$

Hence, passing the turning point lying in the region II we have picked up an extra factor $\exp(-\mathrm{i}\pi/2)$. Since $S''(x_4) < 0$ and $S''(x_1) > 0$, we pick up another factor of $\exp(-\mathrm{i}\pi/2)$ when we go through region IV and pass the second turning point,

$$\psi_{\mathrm{III}}(x) \to \psi_{\mathrm{I}}(x)\mathrm{e}^{-\mathrm{i}\pi/2}. \tag{C.2}$$

In passing one full turn along the circle, one therefore sees that $\psi_I(x) \to \psi_I(x)\mathrm{e}^{-\mathrm{i}\pi}$. The wavefunction should be single-valued, which means that the exponent should be a multiple of 2π. From equations (B.1) and (B.7), we therefore find that

$$\frac{1}{h}\oint p_x\,\mathrm{d}x - \phi_B - \pi = 2\pi n, \tag{C.3}$$

where $p_x = S'(x)$ is to be found from the Hamilton–Jacobi equation (B.3). The quantity ϕ_B is the Berry phase, defined by

$$\phi_\mathrm{B} = \mathrm{i}\oint \mathrm{d}x \left(\frac{\partial L_0}{\partial p}\right)^{-1}\left(-\chi_0^\dagger \frac{\partial H}{\partial p_x}\frac{\partial \chi_0}{\partial x} + \chi_0^\dagger \frac{\partial \chi_0}{\partial p_x}\frac{\partial L_0}{\partial x} + \frac{1}{2}\frac{\partial^2 L_0}{\partial p \partial x}\right). \tag{C.4}$$

Equation (C.3) can be rewritten as the Bohr–Sommerfeld quantization rule

$$\frac{1}{2\pi}\oint p_x\,\mathrm{d}x = h\left(n + \frac{1}{2} + \frac{\phi_\mathrm{B}}{2\pi}\right). \tag{C.5}$$

Looking back at the above derivation one sees that the term $1/2$ can be written as $\nu/4$, where ν is the number of turning points (the Maslov index in this particular case) [41].

Appendix D. Asymptotic expansions of parabolic cylinder functions in different Stokes sectors

For completeness we place in this section the asymptotic expansions of the parabolic cylinder functions in different Stokes sectors at $|z| \to \infty$ according to [46]:

$$D_\nu(z) \sim \begin{cases} \mathrm{e}^{-z^2/4}z^\nu(1+O[z^{-2}]), & -\pi/2 < \arg(z) \leqslant \pi/2, \\ \mathrm{e}^{-z^2/4}z^\nu(1+O[z^{-2}]) - \frac{\mathrm{e}^{z^2/4-\mathrm{i}\pi\nu}\sqrt{2\pi}z^{-\nu-1}}{\Gamma(-\nu)}(1+O[z^{-2}]), & \\ \qquad\qquad \arg(z) \leqslant -\pi/2, & \\ \mathrm{e}^{-z^2/4}z^\nu(1+O[z^{-2}]) - \frac{\mathrm{e}^{z^2/4+\mathrm{i}\pi\nu}\sqrt{2\pi}z^{-\nu-1}}{\Gamma(-\nu)}(1+O[z^{-2}]), & \\ \qquad\qquad \arg(z) > \pi/2. & \end{cases} \tag{D.1}$$

We assume that $-\pi < \arg(z) < \pi$.

References

[1] Geim A K and Novoselov K S 2007 The rise of graphene *Nature Mater.* **6** 183
[2] Katsnelson M I 2007 Graphene: carbon in two dimensions *Mater. Today* **10** 20
[3] Castro Neto A H, Guinea F, Peres N M R, Novoselov K S and Geim A K 2009 The electronic properties of graphene *Rev. Mod. Phys.* **81** 109
[4] Beenakker C W J 2008 Colloquium: Andreev reflection and Klein tunneling in graphene *Rev. Mod. Phys.* **80** 1337
[5] Geim A K 2009 Graphene: status and prospects *Science* **324** 1530
[6] Peres N M R 2010 Colloquium: the transport properties of graphene: an introduction *Rev. Mod. Phys.* **82** 2673
[7] Vozmediano M A H, Katsnelson M I and Guinea F 2010 Gauge fields in graphene *Phys. Rep.* **496** 109
[8] Katsnelson M I, Novoselov K S and Geim A K 2006 Chiral tunnelling and the Klein paradox in graphene *Nature Phys.* **2** 620–5
[9] Klein O 1929 Die reflexion von elektronen an einem potentialsprung nach der relativistischen dynamik von Dirac *Z. Phys.* **53** 157–65
[10] Calogeracos A and Dombey N 1999 History and physics of the Klein paradox *Contemp. Phys.* **40** 313
[11] Dombey N and Calogeracos A 1999 Seventy years of the Klein paradox *Phys. Rep.* **315** 41
[12] Greiner W and Schramm S 2008 Resource letter QEDV-1: the QED vacuum *Am. J. Phys.* **76** 509
[13] Vonsovsky S V and Svirsky M S 1993 The Klein paradox and the zitterbewegung of an electron in a field with a constant scalar potential *Usp. Fiz. Nauk* **163** 115
[14] Su R-K, Siu G G and Chou X 1993 Barrier penetration and Klein paradox *J. Phys. A: Math. Gen.* **26** 1001
[15] Stratton J A 1941 *Electromagnetic Theory* (New York: McGraw-Hill)
[16] Landau L D and Peierls R 1931 Erweiterung des unbestimmtheitsprinzips für die relativistische quantentheorie *Z. Phys.* **69** 56
[17] Berestetskii V B, Lifshitz E M and Pitaevskii L P 1971 *Relativistic Quantum Theory* (*Course of Theoretical Physics* vol 4) (Oxford: Pergamon)
[18] Calogeracos A, Dombey N and Imagawa K 1996 Spontaneous fermion production by a supercritical potential well *Phys. At. Nucl.* **59** 1275
[19] Krekora P, Su Q and Grobe R 2005 Klein paradox with spin-resolved electrons and positrons *Phys. Rev.* A **72** 064103
[20] Ando T, Nakanishi T and Saito R 1998 Berry's phase and absence of back scattering in carbon nanotubes *J. Phys. Soc. Japan* **67** 2857
[21] Yennie D R, Ravenhall D G and Wilson R N 1954 Phase-shift calculation of high-energy electron scattering *Phys. Rev.* **95** 500
[22] Lifshitz I M, Gredeskul S A and Pastur L A 1998 *Introduction to the Theory of Disordered Systems* (New York: Wiley)
[23] Newton R G 1966 *Scattering Theory of Waves and Particles* (New York: McGraw-Hill)
[24] Greiner W, Mueller B and Rafelski J 1985 *Quantum Electrodynamics of Strong Fields* (Berlin: Springer)
[25] Grib A A, Mamaev S V and Mostepanenko V M 1994 *Vacuum Effects in Strong Fields* (St Petersburg: Friedmann)
[26] Stander N, Huard B and Goldhaber-Gordon D 2009 Evidence for Klein tunneling in graphene p–n junctions *Phys. Rev. Lett.* **102** 026807
[27] Young A F and Kim P 2009 Quantum interference and Klein tunnelling in graphene heterojunctions *Nature Phys.* **5** 222
[28] Esaki L 1958 New phenomenon in narrow germanium para-normal-junctions *Phys. Rev.* **109** 603
[29] Meyer J R, Hoffman C A, Bartoli F J and Rammohan L R 1995 Type-II quantum-well lasers for the midwavelength infrared *Appl. Phys. Lett.* **67** 757
[30] Teissier R, Finley J J, Skolnick M S, Cockburn J W, Pelouard J-L, Grey R, Hill G, Pate M-A and Planel R 1996 Experimental determination of Γ-X intervalley transfer mechanisms in GaAs/AlAs heterostructures *Phys. Rev.* B **54** 8329
[31] Dresselhaus M S and Dresselhaus G 2002 Intercalation compounds of graphite *Adv. Phys.* **51** 1
[32] Kuzmenko A B, Crassee I, van der Marel D, Blake P and Novoselov K S 2009 Determination of the gate-tunable band gap and tight-binding parameters in bilayer graphene using infrared spectroscopy *Phys. Rev.* B **80** 165406
[33] McCann E and Falko V I 2006 Landau-level degeneracy and quantum Hall effect in a graphite bilayer *Phys. Rev. Lett.* **96** 086805
[34] Novoselov K S, McCann E, Morozov S V, Falko V I, Katsnelson M I, Zeitler U, Jiang D, Schedin F and Geim A K 2006 Unconventional quantum Hall effect and Berry's phase of 2π in bilayer graphene *Nature Phys.* **2** 177

[35] McCann E, Abergel D S L and Falko V I 2007 Electrons in bilayer graphene *Solid State Commun.* **143** 110
[36] Foldy L and Wouthuysen S 1950 On the Dirac theory of spin 1/2 particles and its non-relativistic limit *Phys. Rev.* **78** 29–36
[37] Blount E I 1961 Bloch electrons in a magnetic field *Phys. Rev.* **126** 1636–53
[38] Berlyand L V and Dobrokhotov Y S 1987 Operator separation of variables in problems of short-wave asymptotics for differential equations with rapidly oscillating coefficients *Dokl. Akad. Nauk SSSR* **296** 80–4
[39] Belov V V, Dobrokhotov Y S and Tudorovskiy Y T 2006 Operator separation of variables for adiabatic problems in quantum and wave mechanics *J. Eng. Math.* **55** 183–237
[40] Maslov V P 1972 *Perturbation Theory and Asymptotic Methods* (Paris: Dunod)
[41] Maslov V P and Fedoryuk M V 1981 *Semi-Classical Approximation in Quantum Mechanics* (Dordrecht: Reidel)
[42] Shytov A V, Rudner M S and Levitov L S 2008 Klein backscattering and Fabry–Pérot interference in graphene heterojunctions *Phys. Rev. Lett.* **101** 156804
[43] Carmier P and Ullmo D 2008 Berry phase in graphene: semiclassical perspective *Phys. Rev.* B **77** 245413
[44] Cheianov V V and Fal'ko V I 2006 Selective transmission of Dirac electrons and ballistic magnetoresistance of n–p junctions in graphene *Phys. Rev.* B **74** 041403
[45] Abramowitz M and Stegun I A (ed) *Handbook of Mathematical Functions with Formulas, Graphs, and Mathematical Tables* (New York: Dover) chapter 19, p 686
[46] http://functions.wolfram.com/HypergeometricFunctions/ParabolicCylinderD
[47] Evgrafov M A and Fedoryuk M V 1966 Asymptotic behaviour as $\lambda \to \infty$ of the solution of the equation $w''(z)p(z,)w(z) = 0$ in the complex z-plane *Russ. Math. Surv.* **21** 1
[48] Landau L D and Lifshitz E M 1977 *Quantum Mechanics, Non-relativistic Theory* (*Course of Theoretical Physics* vol 3) 2nd edn (Oxford: Pergamon)
[49] Heading J 1962 *An Introduction to Phase-Integral Methods (Methuen's Monographs on Physical Subjects)* (Methuen: London) (a Russian translation with an appendix by V P Maslov on the WKB method in the multi-dimensional case was published in 1965 by MIR, Moscow)
[50] Fröman N and Fröman P O 1962 *JWKB Approximation, Contributions to the Theory* (Amsterdam: North-Holland)
[51] Berry M V and Mount K E 1972 Semiclassical approximations in wave mechanics *Rev. Prog. Phys.* **35** 315–97
[52] Fröman N and Fröman P O 2002 *Physical Problems Solved by the Phase-Integral Method* (Cambridge: Cambridge University Press)
[53] Goldstein H, Poole C P and Safko J L 2002 *Classical Mechanics* 3rd edn (San Fransisco, CA: Addison-Wesley)